

TECH
LIBRARY
KAFB, NM
0066288

NACA TN 3240

NATIONAL ADVISORY COMMITTEE FOR AERONAUTICS

TECHNICAL NOTE 3240

THEORETICAL CALCULATIONS OF THE LATERAL STABILITY
DERIVATIVES FOR TRIANGULAR VERTICAL TAILS
WITH SUBSONIC LEADING EDGES TRAVELING
AT SUPERSONIC SPEEDS

By Percy J. Bobbitt

Langley Aeronautical Laboratory
Langley Field, Va.

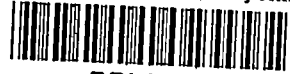


Washington

December 1954

AFM2C

TECHNICAL
NOTE 3240
AFM2C



0066288

N

NATIONAL ADVISORY COMMITTEE FOR AERONAUTICS

TECHNICAL NOTE 3240

THEORETICAL CALCULATIONS OF THE LATERAL STABILITY

DERIVATIVES FOR TRIANGULAR VERTICAL TAILS

WITH SUBSONIC LEADING EDGES TRAVELING

AT SUPERSONIC SPEEDS

By Percy J. Bobbitt

SUMMARY

Pressure-distribution expressions and stability derivatives have been derived by use of linear theory for zero-end-plate triangular vertical tails with subsonic leading edges performing rolling, yawing, and constant-lateral-acceleration motions. Corresponding results for the sideslip motion, most of which have been previously reported, are also included herein.

Consideration is given to the effect of end plates on the forces acting on the vertical tail. Stability-derivative formulas for a vertical tail in the presence of a complete end plate obtained from wing results are also presented, together with a suggested approximation for partial-end-plate effects.

The aerodynamic damping of the lateral oscillation in yaw is approximated to the first order in frequency from the damping of the yawing and constant-lateral-acceleration motions. Illustrative variations of the stability derivatives for the special case of the half-delta tail for all the motions considered are included.

INTRODUCTION

Information available at present that pertains to the aerodynamic forces acting on various tail arrangements is, in many instances, insufficient to allow the accurate prediction of the lateral dynamic behavior of aircraft traveling at supersonic speeds. Theoretical results now available are, for the most part, concerned with tail configurations either in a rolling or in a sideslip attitude (see refs. 1 to 11).

For the sideslip motion, the effects of Mach number and aspect ratio on the aerodynamic loads of a number of tail configurations with both one and two planes of cross-sectional symmetry have already been investigated extensively. The same effects on tail arrangements in a rolling motion have also received considerable attention but it has, in the main, been directed toward tails with two planes of symmetry such as cruciform arrangements. Additional theoretical analysis devoted to the evaluation of the Mach number and aspect-ratio effects on the forces and moments acting on tail systems in roll with one plane of cross-sectional symmetry is required.

Tail arrangements performing a steady yawing motion or a constant-lateral-acceleration motion have received little attention to date in the literature. Yet the forces and moments produced by these motions are by no means negligible, and some indication of their magnitudes is necessary, particularly at supersonic speeds, in order to evaluate their relative importance on lateral stability.

The primary purpose of this paper is to provide the pressure-distribution expressions and corresponding stability derivatives for isolated triangular vertical tails with subsonic leading edges performing yawing, rolling, and constant-lateral-acceleration motions. Some of these results in turn are used to approximate to the first order in frequency the damping of the vertical tail oscillating in yaw (one degree of freedom).

A secondary objective, in view of the geometric nonplanar characteristics of tail arrangements, is to give consideration to the estimation of the mutual aerodynamic interference that exists between the vertical and horizontal tails. In this connection the stability derivatives for the vertical tail in the presence of a complete end plate have been included.

For completeness, results for the no-end-plate and complete-end-plate vertical tails in a sideslip motion obtained from references 9 and 11 are also presented.

SYMBOLS

The positive directions of the forces, moments, velocities, and angles are shown in figure 1.

x,y,z coordinates of field point

$$\theta = \frac{z}{x}$$

x_1, z_1	coordinates of doublet
$\sigma = \frac{z_1}{x_1}$	
x_0, z_0	distances origin is displaced relative to tail apex
t	time
u	incremental velocity in x-direction
v	y-component of velocity
w	z-component of velocity
V	free-stream velocity
a	speed of sound
p	rolling angular velocity
r	yawing angular velocity
α	angle of attack
$\dot{\alpha}$	rate of change of α with time
β	sideslip angle
$\dot{\beta}$	rate of change of β with time
ρ	fluid density
q	free-stream dynamic pressure, $\frac{1}{2}\rho V^2$
ΔP	pressure difference between opposite sides of a surface
$B = \sqrt{\left(\frac{V}{a}\right)^2 - 1}$	
κ	constant determining degree of homogeneity of quasi-conical velocity field
ϕ	velocity-potential function
ϕ_D	potential of supersonic doublet distribution

ϕ_L	potential of line of doublets
x	steady-state potential corresponding to unit angle of sideslip
ψ	steady-state potential corresponding to unit yawing velocity about z-axis
$A(x, z)$	doublet-strength function
$f(\sigma)$	line-doublet-distribution function
b_v	span of vertical tail
S_v	vertical-tail area
A_v	aspect ratio of vertical tail, $\frac{b_v^2}{S_v} = \frac{2C}{1 - R}$
ϵ	apex angle of tail
C	tangent of apex angle
R	ratio of slope of leading edge of tail to slope of trailing edge of tail, $1 - \frac{2BC}{BA_v}$
k	$k = \frac{1 - \sqrt{1 - B^2C^2}}{BC}$
$E'(BC)$	complete elliptic integral of second kind with modulus $\sqrt{1 - B^2C^2}$, $\int_0^{\pi/2} \sqrt{1 - (1 - B^2C^2)\sin^2 n} dn$
$K'(BC)$	complete elliptic integral of first kind with modulus $\sqrt{1 - B^2C^2}$, $\int_0^{\pi/2} \frac{dn}{\sqrt{1 - (1 - B^2C^2)\sin^2 n}}$
$E'(k)$	complete elliptic integral of second kind with modulus $\sqrt{1 - k^2}$, $\int_0^{\pi/2} \sqrt{1 - (1 - k^2)\sin^2 n} dn$

$K'(k)$ complete elliptic integral of first kind with modulus

$$\sqrt{1 - k^2} \int_0^{\pi/2} \frac{dn}{\sqrt{1 - (1 - k^2) \sin^2 n}}$$

M, N, M', N' constants

$\bar{N} = NBC$

η infinitesimally small quantity

$$G(BC) = \frac{1 - B^2 C^2}{(1 - 2B^2 C^2) E'(BC) + B^2 C^2 K'(BC)}$$

$$\gamma = \frac{x - B^2 z \sigma}{\sqrt{1 - B^2 \sigma^2} \sqrt{x^2 - B^2(y^2 + z^2)}}$$

$$\xi = \lim_{\frac{\beta y}{x} \rightarrow 0} \gamma = \frac{1 - B^2 \sigma \theta}{\sqrt{1 - B^2 \sigma^2} \sqrt{1 - B^2 \theta^2}}$$

C_l rolling-moment coefficient, $\frac{\text{Rolling moment}}{q S_v b_v}$

C_n yawing-moment coefficient, $\frac{\text{Yawing moment}}{q S_v b_v}$

C_Y side-force coefficient, $\frac{\text{Side force}}{q S_v}$

$$C_{l_\beta} = \left(\frac{\partial C_l}{\partial \beta} \right)_{\beta \rightarrow 0}$$

$$C_{l_p} = \left(\frac{\partial C_l}{\partial \frac{pb_v}{V}} \right)_{p \rightarrow 0}$$

$$C_{l_r} = \left(\frac{\partial C_l}{\partial \frac{rb_v}{V}} \right)_{r \rightarrow 0}$$

$$C_{l\dot{\beta}} = \left(\frac{\partial C_l}{\partial \dot{\beta} b_v} \right)_{\dot{\beta} \rightarrow 0}$$

$$C_{n\dot{\beta}} = \left(\frac{\partial C_n}{\partial \dot{\beta}} \right)_{\dot{\beta} \rightarrow 0}$$

$$C_{n_p} = \left(\frac{\partial C_n}{\partial \frac{pb_v}{V}} \right)_{p \rightarrow 0}$$

$$C_{n_r} = \left(\frac{\partial C_n}{\partial \frac{rb_v}{V}} \right)_{r \rightarrow 0}$$

$$C_{n\dot{\beta}} = \left(\frac{\partial C_n}{\partial \dot{\beta} b_v} \right)_{\dot{\beta} \rightarrow 0}$$

$$C_{Y\dot{\beta}} = \left(\frac{\partial C_Y}{\partial \dot{\beta}} \right)_{\dot{\beta} \rightarrow 0}$$

$$C_{Y_p} = \left(\frac{\partial C_Y}{\partial \frac{pb_v}{V}} \right)_{p \rightarrow 0}$$

$$C_{Y_r} = \left(\frac{\partial C_Y}{\partial \frac{rb_v}{V}} \right)_{r \rightarrow 0}$$

$$C_{Y\dot{\beta}} = \left(\frac{\partial C_Y}{\partial \dot{\beta} b_v} \right)_{\dot{\beta} \rightarrow 0}$$

Subscripts:

p	rolling condition
r	yawing condition
β	sideslip condition
$\dot{\beta}$	constant-lateral-acceleration condition
0	zero-end-plate configuration
C	complete-end-plate configuration
P	partial-end-plate configuration

SCOPE

Derived in this paper are expressions for the surface pressure distributions on isolated triangular vertical tails performing yawing, rolling, and constant-lateral-acceleration motions. These pressure expressions have in turn been used to calculate the stability derivatives associated with the side force, yawing moment, and rolling moment due to constant yawing (C_{Yr} , C_{nr} , and C_{lr}), constant rolling (C_{Yp} , C_{np} , and C_{lp}), and constant lateral acceleration ($C_{Y\dot{\beta}}$, $C_{n\dot{\beta}}$, and $C_{l\dot{\beta}}$). Also presented are the aerodynamic coefficients $C_{Y\beta}$, $C_{n\beta}$, and $C_{l\beta}$ obtained from the sideslip pressure-distribution expression given in reference 11. Stability derivatives presented for the vertical tail of figure 1 mounted on a complete end plate are $C_{Y\beta}$, $C_{n\beta}$, C_{Yr} , C_{nr} , $C_{Y\dot{\beta}}$, and $C_{n\dot{\beta}}$. The equation of $C_{l\beta}$ for a triangular-vertical-tail-end-plate combination may be derived from the pressure distributions given in reference 9. This equation has not been determined and only curves of $C_{l\beta}$ taken from reference 9 for a vertical-tail-complete-end-plate combination with trailing edges perpendicular to the root chord (see fig. 2) are presented.

The stability derivatives presented herein are valid within the limits of linear theory for a range of Mach numbers for which the leading edge is subsonic and the trailing edge supersonic. Variations of all the stability derivatives with the parameter BC are presented for a triangular vertical tail with zero trailing-edge sweep (half-delta tail).

ANALYSIS

The axes system used in the analysis and the positive directions of the forces, moments, velocities, and angles are shown in figure 1. The positive directions of the forces and moments in the analysis system have been fixed to conform to the positive directions of the forces and moments in the stability axes system (see fig. 3(a)). The stability-derivative expressions are derived in the body of the report with respect to the analysis system whose origin is at the apex of the tail. Transfer formulas are presented, however, which allow these derivative expressions to be determined for a system of axes whose origin is displaced longitudinally and vertically with respect to the apex of the vertical tail. (See fig. 3(b).)

The ensuing analysis is based on linearized theory and the results are restricted to vertical tails of zero camber with surfaces of vanishingly small thickness. These conditions implicitly stipulate that the results are valid only for small angles of sideslip, small rates of change of the sideslip angle with time ($\dot{\beta}$ motion), and low rates of rolling and yawing.

Throughout the analysis, when the potential of a surface in the xz -plane is referred to, it is considered to be the surface potential on the side of the vertical tail whose outward normal is in the positive y -direction; that is,

$$\phi = \phi(x, 0^+, z)$$

and for a surface in the xy -plane,

$$\phi = \phi(x, y, 0^+)$$

Pressure differences between opposite sides of a surface are formulated as follows:

For a surface in the xy -plane,

$$\Delta P = P(x, y, 0^+) - P(x, y, 0^-)$$

and for a surface in the xz -plane,

$$\Delta P = P(x, 0^+, z) - P(x, 0^-, z)$$

Determination of Pressure-Distribution Expressions

for Yawing and Rolling Motions

A method for solving supersonic-flow boundary-value problems governed by the classical, linearized, partial-differential equation

$$B^2 \frac{\partial^2 \phi}{\partial x^2} - \frac{\partial^2 \phi}{\partial y^2} - \frac{\partial^2 \phi}{\partial z^2} = 0 \quad (1)$$

has been developed in reference 12 and an application to rolling and pitching triangular wings is given in reference 13. This method allows the prediction of the disturbance-potential function ϕ , and hence the pressure distribution, for planar lifting surfaces. The analysis given in reference 13 is briefly summarized herein and is applied to the determination of the pressure distributions and associated forces and moments acting on a triangular vertical tail surface (fig. 1) performing rolling and yawing motions. (Yawing in the xz-plane is analogous to pitching in the xy-plane.)

The determination of the form of the velocity potential.— As is well-known, the potentials of both the supersonic source and the supersonic doublet and their distributions represent solutions of equation (1). For the determination of the potentials and pressure distributions of lifting surfaces of the type considered herein, that is, for lifting surfaces with subsonic leading edges, it is well-known that a distribution of doublets that uniquely satisfies the prescribed boundary conditions must be determined. These boundary conditions on the vertical tail for the motions to be considered herein are as follows:

On the rolling vertical tail,

$$v = p_z = xp \frac{z}{x} = xp\theta \quad (2)$$

and on the yawing vertical tail,

$$v = -rx \quad (3)$$

In addition, the following relations must be valid on the surfaces of the tail:

For the rolling motion,

$$\frac{\partial \left(\frac{v}{x}\right)_p}{\partial \theta} = p \quad (4)$$

$$\frac{\partial^2 \left(\frac{v}{x}\right)_p}{\partial \theta^2} = 0 \quad (5)$$

and for the yawing motion,

$$\frac{\partial \left(\frac{v}{x}\right)_r}{\partial \theta} = 0 \quad (6)$$

$$\frac{\partial^2 \left(\frac{v}{x}\right)_r}{\partial \theta^2} = 0 \quad (7)$$

The potential in space produced by a distribution of doublets, for example, in the xz-plane, with the doublet axes normal to the plane is

$$\phi_D(x, y, z) = \frac{\partial}{\partial y} \iint_S \frac{-A(x_1, z_1) dx_1 dz_1}{\sqrt{(x - x_1)^2 - B^2(z - z_1)^2 - B^2 y^2}} \quad (8)$$

where the area S is the region of the xz-plane intercepted by the forecone from the field point (x, y, z) .

The potential on the surface carrying the doublet distribution is given by

$$\phi_D(x, z)_{y=0} = \lim_{y \rightarrow \pm 0} \left[\frac{\partial}{\partial y} \iint_S \frac{-A(x_1, z_1) dx_1 dz_1}{\sqrt{(x - x_1)^2 - B^2(z - z_1)^2 - B^2 y^2}} \right]$$

As stated in reference 13, this surface potential is directly proportional to the doublet-strength function $A(x, z)$; that is,

$$\phi_D(x, z)_{y=\pm 0} = \pm \pi A(x, z) \quad (9)$$

The surface-pressure velocity $u(x, z)$ therefore is

$$u(x, z)_{y=\pm 0} = \frac{\partial \phi_D(x, z)_{y=\pm 0}}{\partial x} = \pm \pi \frac{\partial A(x, z)}{\partial x} \quad (10)$$

and the linearized lifting-pressure coefficient

$$\frac{\Delta P}{q} = \frac{4u(x, z)_{y=+0}}{V} \quad (11)$$

may be written as

$$\frac{\Delta P}{q} = \frac{4\pi}{V} \frac{\partial A(x, z)}{\partial x} \quad (12)$$

The problem to be considered in this paper is one in which the sidewash on the surface is prescribed (see eqs. (2) and (3)) and the surface velocity potential has to be determined. The doublet-strength function $A(x, z)$ then is an unknown and the determination of this quantity requires in general the solution of an integral equation. In some cases the general form of the surface-potential function $A(x, z)$ is known or can be obtained by inverting an integral equation. The problem then resolves simply into an evaluation of the arbitrary constants of the general solution by making use of the prescribed boundary conditions.

Brown and Adams in their analysis of triangular wings with subsonic leading edges (ref. 13) were able to determine the function $A(x, z)$ for these wings undergoing various motions by utilizing the concept that the conical properties of the produced flow gave rise to potentials and pressures in the crossflow planes that were similar in form to the potentials and pressures acting on flat finite segments in a two-dimensional flow; these segments correspond to a section of the wing in any crossflow plane. This remarkable connection between linearized supersonic conical flow and incompressible two-dimensional flow is discussed by Busemann in reference 14.

A more general and rigorous approach to obtain the doublet-strength function may be formulated from an analysis presented in a later paper by Lomax and Heaslet (ref. 15) dealing also with conical and the so-called quasi-conical problems. In this analysis a general surface-pressure-coefficient expression has been determined for planar lifting surfaces with prescribed boundary conditions of the form

$$v \sim x^\kappa g\left(\frac{z}{x}\right) \quad (13)$$

This expression is

$$\frac{\Delta P}{q} = \left(\frac{x}{B}\right)^\kappa \sum_{i=0}^{\kappa+1} \frac{b_i \theta^i}{\sqrt{(C - \theta)(\theta - C_1)}} \quad (14)$$

where b_i are constants, $\theta = \frac{z}{x}$, κ is determined by the boundary-condition equation (eq. (13)), and C and C_1 are the tangents of the apex angles of the two panels of the lifting surface. When $C_1 = C$, the lifting surface is symmetrical about the common root chord of the two panels, and when $C_1 \neq C$, the lifting surface is asymmetrical about this chord. From equation (12), which relates the function $A(x, z)$ to the pressure coefficient, and equation (9) the form of $A(x, z)$ or, synonymously, the form of the surface potential, may be obtained by a simple integration. It should be mentioned at this point that reference 15 presents a method for deriving the arbitrary constants b_i in the pressure coefficient (eq. (14)). This method is related to that of reference 13 which concerns itself with obtaining the arbitrary constants in the velocity potential.

By application of equation (14) to the boundary problem of the vertical tail sketched in figure 1 ($C_1 = 0$) and by noting from the prescribed boundary conditions (see eqs. (2) and (3)) that $\kappa = 1$, the pressure coefficient for both the yawing and rolling motions is

$$\frac{\Delta P}{q} = \frac{x}{B} \frac{b_0 + b_1 \theta + b_2 \theta^2}{\sqrt{(C - \theta)\theta}} \quad (15)$$

The constant b_0 in this expression must be set equal to zero in order to satisfy the condition that along the streamwise edge the pressure must be zero.

The velocity potential on the vertical tail surface is easily obtainable from the pressure expression by the formula

$$\phi = \frac{V}{4} \int_{L.E.}^x \frac{\Delta P}{q} dx_1$$

and has been found to be

$$\phi = \pi x^2 f\left(\frac{z}{x}\right) \quad (16)$$

where

$$f\left(\frac{z}{x}\right) = f(\theta) = (M\theta + NC)\sqrt{\theta(C - \theta)} \quad (17)$$

The arbitrary constants in the so-called distribution function $f(\theta)$ are, in terms of b_1 and b_2 ,

$$M = \frac{V}{2\pi B} \left(\frac{2b_1}{3C^2} + \frac{b_2}{C} \right)$$

$$N = \frac{V}{2\pi B} \frac{b_1}{3C^2}$$

By relating equation (16) to equation (9), the doublet-strength function $A(x, z)$ is seen to be

$$A(x, z) = x^2 f\left(\frac{z}{x}\right) \quad (18)$$

A comparison of the potential of equations (16) and (17) and the potential obtained for the slender, rolling, vertical tail reported in reference 5 shows, as expected, that both are of the same form.

Evaluation of the constants M and N.—The constants M and N in the expressions for the velocity potential given by equations (16) and (17) are still to be determined. As indicated previously, the expression for the pressure coefficient, and hence the velocity potential, can be determined completely through an application of the procedures developed in reference 15; however, many of the integrations and integrating procedures required in the method in reference 15 were already known to the author at the inception of this project and, for

this reason, the analysis herein to determine the constants M and N closely parallels the procedures discussed in reference 13.

The determination of the constants M and N depends upon satisfying the boundary conditions associated with the vertical tail for the rolling and yawing motions. These boundary conditions are given by equations (2) to (7). The needed expressions for the prescribed velocities and their derivatives with respect to θ in terms of the distribution function $f(\sigma)$ are derived in appendix A.

For the rolling motion the constants M and N may be obtained by replacing $f(\sigma)$ by its equivalent (eq. (17)) in the equations given in appendix A for v/x and $\frac{\partial(v/x)}{\partial\theta}$ and then applying the boundary conditions given by equations (2) and (4). When the integrations have been performed, the resulting equations may be solved simultaneously for M_p and N_p . The yawing constants are obtained in a like manner with equations (3) and (6) replacing equations (2) and (4), respectively.

In the calculation of the quantities v/x and $\frac{\partial(v/x)}{\partial\theta}$, any value of θ may be considered. It is advantageous for integration purposes to let this value of θ be zero. However, since one of the limits of integration is zero and since in several of the integrands a singular point exists at $\theta = \sigma = 0$, the integrations in which these singularities occur must be performed for θ arbitrary and then θ is set equal to zero.

Substituting equation (17) into equation (A4) gives, for θ equal to zero,

$$\begin{aligned} \frac{v}{x} = & \frac{1}{B} \int_0^{BC} \left[\frac{-3(MB\sigma + NBC)\sqrt{B\sigma(BC - B\sigma)} \tanh^{-1} \sqrt{1 - B^2\sigma^2}}{(1 - B^2\sigma^2)^{5/2}} + \frac{2(MB\sigma + NBC)\sqrt{B\sigma(BC - B\sigma)}}{(1 - B^2\sigma^2)^2} \right] d(B\sigma) + \\ & \lim_{\theta \rightarrow 0} \left\{ \lim_{\eta \rightarrow 0} \left[\frac{1}{B} \int_0^{B(\theta-\eta)} \frac{(MB\sigma + NBC)\sqrt{B\sigma(BC - B\sigma)}(1 - B^2\sigma\theta)^2 \sqrt{1 - B^2\theta^2}}{(1 - B^2\sigma^2)^2 (B\sigma - B\theta)^2} d(B\sigma) + \right. \right. \right. \\ & \left. \left. \left. \frac{1}{B} \int_{B(\theta+\eta)}^{BC} \frac{(MB\sigma + NBC)\sqrt{B\sigma(BC - B\sigma)}(1 - B^2\sigma\theta)^2 \sqrt{1 - B^2\theta^2}}{(1 - B^2\sigma^2)^2 (B\sigma - B\theta)^2} d(B\sigma) - \right. \right. \right. \\ & \left. \left. \left. \frac{2(MB\theta + NBC)\sqrt{B\theta(BC - B\theta)}\sqrt{1 - B^2\theta^2}}{B^2\eta} \right] \right\} \end{aligned} \quad (19)$$

Carrying out the integrations in equation (19) yields

$$\frac{v}{x} = \frac{-\pi}{B\sqrt{1+k^2}(1-k^2)^2} \left\{ K'(k) \left[2k^3 M + \bar{N}k^2(1+k^2) \right] - E'(k) \left[Mk(1+k^2) - \bar{N}(1-4k^2+k^4) \right] \right\} \quad (20)$$

where

$$k = \frac{1 - \sqrt{1 - B^2 C^2}}{BC} \quad (21)$$

and

$$\bar{N} = NBC = N \frac{2k}{1+k^2}$$

These integrations were accomplished with the aid of the tables in references 16 and 17 and are discussed in appendix B.

Substituting the distribution function into equation (A5) results in, for θ approaching zero,

$$\begin{aligned} \frac{\partial(v/x)}{\partial\theta} &= \int_0^{BC} \left[\frac{3B\sigma(MB\sigma + NBC)\sqrt{B\sigma(BC - B\sigma)} \tanh^{-1}\sqrt{1 - B^2\sigma^2}}{(1 - B^2\sigma^2)^{5/2}} - \frac{3B\sigma(MB\sigma + NBC)\sqrt{B\sigma(BC - B\sigma)}}{(1 - B^2\sigma^2)^2} \right] d(B\sigma) + \\ &\lim_{\theta \rightarrow 0} \left(\lim_{\eta \rightarrow 0} \left\{ \int_0^{B(\theta-\eta)} \left[\frac{B\theta(MB\sigma + NBC)\sqrt{B\sigma(BC - B\sigma)}}{\sqrt{1 - B^2\theta^2}(B\sigma - B\theta)^2} - \frac{(MB\sigma + NBC)\sqrt{B\sigma(BC - B\sigma)}}{\sqrt{1 - B^2\theta^2}(1 - B^2\sigma^2)(B\sigma - B\theta)} + \right. \right. \right. \\ &\left. \left. \left. \frac{2(MB\sigma + NBC)\sqrt{B\sigma(BC - B\sigma)}\sqrt{1 - B^2\theta^2}}{(B\sigma - B\theta)^3} \right] d(B\sigma) + \int_{B(\theta+\eta)}^{BC} \left[\frac{B\theta(MB\sigma + NBC)\sqrt{B\sigma(BC - B\sigma)}}{\sqrt{1 - B^2\theta^2}(B\sigma - B\theta)^2} - \right. \right. \\ &\left. \left. \left. \frac{(MB\sigma + NBC)\sqrt{B\sigma(BC - B\sigma)}}{\sqrt{1 - B^2\theta^2}(1 - B^2\sigma^2)(B\sigma - B\theta)} + \frac{2(MB\sigma + NBC)\sqrt{B\sigma(BC - B\sigma)}\sqrt{1 - B^2\theta^2}}{(B\sigma - B\theta)^3} \right] d(B\sigma) - \right. \\ &\left. \left. \left. \frac{2B\theta(MB\theta + NBC)\sqrt{B\theta(BC - BC)}}{B\eta\sqrt{1 - B^2\theta^2}} - \frac{2[-4B^2\theta^2M + B\theta BC(3M - 2N) + NB^2C^2]\sqrt{1 - B^2\theta^2}}{B\eta\sqrt{B\theta(BC - BC)}} \right] \right\} \right) \quad (22) \end{aligned}$$

By performing the integrations in equation (22), the following expression is obtained:

$$\frac{\partial(v/x)}{\partial\theta} = \frac{\pi}{\sqrt{1+k^2(1-k^2)^2}} \left[k^2 K'(k) (M + Mk^2 + 2\bar{N}k) + E'(k) (2Mk^2 - 2M - \bar{N}k - 2Mk^4 - \bar{N}k^3) \right] \quad (23)$$

Consider the rolling case; that is, $M = M_p$, $N = N_p$, and from equations (2) and (4) v/x and $\frac{\partial(v/x)}{\partial\theta}$ are, for $\theta = 0$, equal to 0 and p , respectively. Solving equations (20) and (23) for M_p and N_p , with $\bar{N} = BCN_p = \frac{2k}{1+k^2} N_p$, gives

$$M_p = \frac{-p\sqrt{1+k^2} \left[k^2(1+k^2)K'(k) + (1-4k^2+k^4)E'(k) \right]}{\pi \left[-k^4K'(k)^2 + k^2(1+k^2)K'(k)E'(k) + (2-k^2)(1-2k^2)E'(k)^2 \right]} \quad (24)$$

$$N_p = \frac{p(1+k^2)^{3/2} \left[2k^2K'(k) - (1+k^2)E'(k) \right]}{2\pi \left[-k^4K'(k)^2 + k^2(1+k^2)K'(k)E'(k) + (2-k^2)(1-2k^2)E'(k)^2 \right]} \quad (25)$$

For the yawing case $M = M_r$, $\bar{N} = \frac{2k}{1+k^2} N_r$, and from equations (3) and (6) $\frac{v}{x} = -r$ and $\frac{\partial(v/x)_r}{\partial\theta} = 0$. Solving equations (20) and (23) simultaneously after making these substitutions yields

$$M_r = \frac{Brk\sqrt{1+k^2} \left[2k^2K'(k) - (1+k^2)E'(k) \right]}{\pi \left[-k^4K'(k)^2 + k^2(1+k^2)K'(k)E'(k) + (2-k^2)(1-2k^2)E'(k)^2 \right]} \quad (26)$$

$$N_r = \frac{-Br(1+k^2)^{3/2} [k^2(1+k^2)K'(k) - 2(1-k^2+k^4)E'(k)]}{2\pi k [-k^4K'(k)^2 + k^2(1+k^2)K'(k)E'(k) + (2-k^2)(1-2k^2)E'(k)^2]} \quad (27)$$

It is convenient for plotting purposes and in expressing the aerodynamic coefficients to make the following definitions:

$$\left. \begin{aligned} M_r &= M_r' \frac{Br}{\pi} \\ N_r &= N_r' \frac{Br}{\pi} \\ M_p &= M_p' \frac{p}{\pi} \\ N_p &= N_p' \frac{p}{\pi} \end{aligned} \right\} \quad (28)$$

so that M_r' , N_r' , M_p' , and N_p' are functions of BC only. The variations of these four parameters with BC are shown in figure 4.

The velocity potentials for the rolling and yawing motions, completely defined by the velocity potential (eqs. (16) and (17)) and the constants given in equations (21), (24), (25), (26), (27), and (28), may now be written as

$$\phi_p = px^2(M_p'\theta + N_p'C)\sqrt{\theta(C-\theta)} \quad (29)$$

and

$$\phi_r = Brx^2(M_r'\theta + N_r'C)\sqrt{\theta(C-\theta)} \quad (30)$$

The pressure coefficients for the rolling and yawing motions found from equations (29), (30), (10), and (11) are

$$\left(\frac{\Delta P}{q}\right)_p = \frac{2p}{V} \frac{M_p' Cz^2 + 3C^2 N_p' xz - 2CN_p' z^2}{\sqrt{z(Cx - z)}} \quad (31)$$

and

$$\left(\frac{\Delta P}{q}\right)_r = \frac{2Br}{V} \frac{M_r' Cz^2 + 3C^2 N_r' xz - 2CN_r' z^2}{\sqrt{z(Cx - z)}} \quad (32)$$

Determination of the Surface-Pressure-Distribution Expression

for Constant Lateral Acceleration

The lateral-acceleration $\dot{\beta}$ motion is time dependent and is not governed by equation (1) but by the linearized partial-differential equation for unsteady supersonic flow:

$$B^2 \frac{\partial^2 \phi}{\partial x^2} - \frac{\partial^2 \phi}{\partial y^2} - \frac{\partial^2 \phi}{\partial z^2} + \frac{2V}{a^2} \frac{\partial^2 \phi}{\partial x \partial t} + \frac{1}{a^2} \frac{\partial^2 \phi}{\partial t^2} = 0 \quad (33)$$

The boundary condition for the $\dot{\beta}$ motion on the tail surface, which is approximately in the $y = 0$ plane, is

$$v = \frac{\partial \phi}{\partial y} = \dot{\beta} V t \quad (34)$$

The potential function satisfying equations (33) and (34) may be obtained from the $\dot{\alpha}$ potential function given in reference 18 for a wing in the xy -plane which was in turn obtained from an analysis by Gardner (ref. 19). This potential function is

$$(\phi)_{\dot{\beta}} = -\dot{\beta} \left[\frac{M^2}{B^2} \psi - \left(t - \frac{M^2 x}{VB^2} \right) x \right] \quad (35)$$

where ψ is the steady-state potential corresponding to a unit yawing velocity about the z-axis and x is the steady-state potential corresponding to a unit angle of sideslip. Thus it is seen that the potential function for the β motion may be written in terms of the time-independent solutions already obtained. It should be noted that equation (35) differs from the formula given in reference 18 by two negative signs, one before the whole expression and one before the second term within the brackets. These two sign differences are necessary to account for the fact that the boundary conditions for the β and $\dot{\beta}$ motions

$$v = \beta V$$

$$\dot{v} = \dot{\beta} V t$$

are opposite in sign to those for the α and $\dot{\alpha}$ motions

$$w = -\alpha V$$

$$\dot{w} = -\dot{\alpha} V t$$

These sign differences on the boundary conditions for the analogous motions require that their potentials and pressures be of opposite sign.

The pressure distribution for a time-dependent motion at the time $t = 0$ from the linearized Bernoulli's equation is

$$\frac{\Delta P}{q} = 2\rho \left(V \frac{\partial \phi}{\partial x} + \frac{\partial \phi}{\partial t} \right) \quad (36)$$

Equation (36) in conjunction with equation (35) yields

$$\begin{aligned} \left(\frac{\Delta P}{q} \right)_\beta &= -2\rho V \dot{\beta} \left(\frac{M^2}{B^2} \frac{\partial \psi}{\partial x} + \frac{M^2 x}{VB^2} \frac{\partial x}{\partial x} + \frac{x}{VB^2} \right) \\ &= -\frac{\dot{\beta}}{B^2} \left[M^2 \left(\frac{\Delta P}{q} \right)_{r=1} + M^2 x \left(\frac{\Delta P}{q} \right)_{\beta=1} + 2\rho x \right] \end{aligned} \quad (37)$$

The pressure coefficient for the sideslip motion may be obtained from reference 11 as

$$\left(\frac{\Delta P}{q}\right)_\beta = - \frac{2\beta z \sqrt{2(1 - \sqrt{1 - B^2 C^2})}}{B E'(k) \sqrt{z(C_x - z)}} \quad (38)$$

The reciprocal of the complete elliptic integral $E'(k)$ appearing in equation (38) is plotted in figure 4 for various values of leading-edge sweep parameter BC .

The expression for x , the only quantity in equation (37) as yet undetermined, can be obtained by substituting equation (38) with $\beta = 1$ into

$$x = \phi_{\beta=1} = \frac{V}{4} \int_{L.E.}^x \left[\frac{\Delta P(x_1, z)}{q} \right]_{\beta=1} dx_1 \quad (39)$$

and carrying out the indicated integration. This process gives

$$x = - \frac{V \sqrt{2(1 - \sqrt{1 - B^2 C^2})} \sqrt{z(C_x - z)}}{B C E'(k)} \quad (40)$$

The pressure coefficient for the β motion is now completely defined by equations (32), (38), (37), and (40).

Force and Moment Coefficients for

Zero-End-Plate Triangular Tails

With the pressure distributions known (eqs. (31), (32), (37), and (38)) the total side force, yawing moment about the apex, and rolling moment about the root chord can be determined for the various motions by the formulas

$$\text{Side force} = q \iint_{S_V} \frac{\Delta P}{q} dz dx \quad (41)$$

$$\text{Yawing moment} = q \iint_{S_V} \frac{\Delta P}{q} x \, dz \, dx \quad (42)$$

$$\text{Rolling moment} = q \iint_{S_V} \frac{\Delta P}{q} z \, dz \, dx \quad (43)$$

The force and moment coefficients and the stability derivatives may be readily obtained from these quantities for zero-end-plate triangular tails and are given in table I.

Force and Moment Coefficients for Complete-End-Plate

Triangular Tails

For the sideslip, yawing, and constant-lateral-acceleration motions the pressures acting on the vertical tail in the presence of a complete end plate are the same as the pressures acting on one-half of a symmetrical wing for the angle-of-attack, pitching, and constant-vertical-acceleration motions, respectively. Each half of this symmetrical wing should have the same plan form as the vertical tail under consideration. For the sideslip motion the pressures on the vertical and horizontal tails with a partial end plate have been reported in reference 9.

Attention is now directed to the effect of end plates on the stability derivatives. For the case of the complete end plate the following vertical-tail derivatives can be obtained from symmetrical-wing results (ref. 20): C_{Y_β} , C_{n_β} , C_{Y_r} , C_{n_r} , C_{Y_β} , and C_{n_β} . The transformations needed to change the symmetrical-wing derivatives into these vertical-tail derivatives are:

$$\text{Expression for } C_{Y_\beta} = -(\text{Expression for } C_{L_\alpha} \text{ with } A \text{ replaced by } 2A_V)$$

$$\text{Expression for } C_{n_\beta} = \frac{-4}{3A_V} \times (\text{Expression for } C_{m_\alpha} \text{ with } A \text{ replaced by } 2A_V)$$

$$\text{Expression for } C_{Y_r} = \frac{2}{3A_V} \times (\text{Expression for } C_{L_q} \text{ with } A \text{ replaced by } 2A_V)$$

$$\text{Expression for } C_{n_r} = \frac{8}{9A_V^2} \times (\text{Expression for } C_{m_q} \text{ with } A \text{ replaced by } 2A_V)$$

$$\text{Expression for } C_{Y\dot{\beta}} = \frac{-2}{3A_v} \times (\text{Expression for } C_{L\dot{\alpha}} \text{ with A replaced by } 2A_v)$$

$$\text{Expression for } C_{n\dot{\beta}} = \frac{-8}{9A_v^2} \times (\text{Expression for } C_{m\dot{\alpha}} \text{ with A replaced by } 2A_v)$$

It should be noted that the above coefficients obtainable from wing results do not include the rolling derivatives $C_{l\dot{\beta}}$, C_{l_r} , and $C_{l\dot{\beta}}$.

Before these aerodynamic coefficients can be evaluated, the rolling moment induced on the end plate must be determined. This moment for the $\dot{\beta}$ motion has been derived in reference 9 but the induced moment for the other two motions are not yet known.

RESULTS AND DISCUSSION

General

Table I contains the formulas for all the p , r , $\dot{\beta}$, and $\dot{\beta}$ stability derivatives for the tail shown in figure 1. Table II presents these derivatives for the half-delta tail (the special case of zero trailing-edge sweep, $A_vB = 2BC$). The variations of these half-delta derivatives with the parameter BC have been plotted in figures 5 to 10. It is evident from tables I and II that the expressions for the $\dot{\beta}$ derivatives have been separated into two component parts, each part being multiplied by a different function of the Mach number parameter B . Each of the components, excluding this factor, is a function of BC . Figures 6, 7, and 8 show the variation of the two parts with BC for each of the $\dot{\beta}$ stability derivatives. Once the Mach number, and hence B , has been specified, the two parts may be combined and the total derivative determined for any given aspect ratio or leading-edge sweep. For the reader's convenience the variations of the $\dot{\beta}$ stability derivatives with Mach number for a number of aspect ratios of the half-delta tail have been plotted in figures 11, 12, and 13. Mach number variations of the other half-delta stability derivatives may be obtained by inspection from their variation with BC .

Side-force and yawing-moment coefficients (as obtained from ref. 20) of the $\dot{\beta}$, $\dot{\beta}$, and r motions for the complete-end-plate vertical tails have been presented in table III. As in the case for the zero end plate, the complete-end-plate stability derivatives for the half-delta tail are presented in a separate table (table IV). The quantities $1/E'(BC)$ and $G(BC)$ appearing in the expressions for the complete-end-plate stability derivatives have been plotted in figure 14.

It should be realized that the force and moments given by equations (41), (42), and (43) and the stability derivatives in tables I, II, III, and IV are for axis locations at the tail apex and root chord. Formulas for the transfer of force and moment coefficients to a body system of axes with the origin displaced a distance x_0 (positive forward) from the tail apex and a distance z_0 (positive downward) from the tail root chord (see fig. 3(b)) are presented in table V.

End-Plate Effect for Sideslip, Yawing, and
Constant-Lateral-Acceleration Motions

Figures 15 to 18 have been prepared to show, for the half-delta tail, the effect of a complete end plate on the side-force and yawing-moment aerodynamic coefficients. It is evident from the large magnitude of the differences between the two limiting cases of a complete end plate and no end plate shown in these figures that a reasonable estimation of the partial-end-plate effects would be highly desirable. End-plate effects for various sizes of horizontal tails for the sideslip motion have been evaluated exactly in reference 9 but are not presented herein. The following approximate formulas for the side-force and yawing-moment stability derivatives based on these partial-end-plate results are suggested:

$$\left. \begin{aligned} (C_{Y_r})_P &= (C_{Y_r})_C - \left[(C_{Y_r})_C - (C_{Y_r})_0 \right] F \\ (C_{n_r})_P &= (C_{n_r})_C - \left[(C_{n_r})_C - (C_{n_r})_0 \right] F \\ (C_{Y_\beta})_P &= (C_{Y_\beta})_C - \left[(C_{Y_\beta})_C - (C_{Y_\beta})_0 \right] F \\ (C_{n_\beta})_P &= (C_{n_\beta})_C - \left[(C_{n_\beta})_C - (C_{n_\beta})_0 \right] F \end{aligned} \right\} \quad (44)$$

where

$$F = \frac{(C_{Y_\beta})_C - (C_{Y_\beta})_P}{(C_{Y_\beta})_C - (C_{Y_\beta})_0}$$

It has been mentioned previously that the effect of end plates on the rolling-moment coefficients has only been evaluated to date for the sideslip motion (ref. 9). By using the results of reference 9, figure 19 has been prepared to show the variation with BC of the stability derivative $C_{l\beta}$ for both a half-delta vertical tail mounted on a complete end plate and an isolated half-delta vertical tail. Also plotted in this figure are the vertical-tail and end-plate contributions to the $C_{l\beta}$ derivative of the complete-end-plate—vertical-tail combination.

Partial-end-plate effects on the rolling-moment coefficients of a vertical tail performing β and r motions cannot be approximated by equations similar to equation (44) since the contribution of the complete end plate to the total rolling moment for these motions is unknown.

End-Plate Effects on Rolling Motion

In the analysis of end-plate effects, complete-end-plate stability derivatives were evaluated by using wing results. This treatment was possible because in the sideslip, yawing, and constant-lateral-acceleration motions the complete end plate acts only to uphold the loading in the same manner as one half of a wing does on the adjacent half. The complete end plate on a rolling vertical tail with, of course, the end plate rolling with the vertical tail causes a sidewash in the plane of the vertical tail which can result in large induced loads, depending on the size of the vertical tail relative to the end plate. This is an end-plate effect very different in nature from the one experienced in the sideslip, yawing, and constant-lateral-acceleration motions where the end plate does not cause a sidewash in the plane of the vertical tail. Clearly then the complete-end-plate boundary can only be established by solving the difficult nonplanar problem. However, some idea of the end-plate effects may be obtained by considering the results shown in reference 5 for slender nonplanar tails. Reference 5 shows that for ratios of vertical-tail span to end-plate span greater than 0.75 the vertical tail does not experience any large changes in loading due to the end plate. This fact suggests the possibility that the Mach number and aspect-ratio effects on the isolated rolling tail (fig. 9) might be applied to the slender, nonplanar, vertical-tail loadings of configurations with ratios of the vertical-tail span to end-plate span greater than 0.75 to yield good estimates (from a theoretical viewpoint) of the side force and yawing moment.

Aspect-ratio and Mach number effects on the rolling isolated tail are apparent from figure 9. The same effects for a rolling wing, which may be thought of as an end plate with a zero-span vertical tail, are illustrated in reference 13. In both cases the magnitude of the forces can be predicted within 10 percent by slender theory up to leading-edge

sweep parameters BC of 0.5. It is not unreasonable to expect that the same agreement would exist for nonplanar tail arrangements as long as the sweep of the leading edges of the panels of the configuration satisfy the condition

$$(B \times \text{Tangent of apex angle of panel}) < 0.5$$

Lateral Oscillatory Motion

It has long been the practice to estimate the aerodynamic damping of longitudinal low-reduced-frequency oscillations of lifting wings from the damping in pitch and damping of the vertical-acceleration motion. An analogous approximation may obviously be used for isolated vertical tail surfaces oscillating laterally in yaw; that is, the lateral damping can be estimated from the results obtained for the yawing and constant-lateral-acceleration motions. This approximation which represents the first-order frequency terms is given by $C_{n_r} - C_{n_\beta}$.

Figure 20 has been prepared to show the variation with Mach number of this damping ($C_{n_r} - C_{n_\beta}$) for half-delta tails of aspect ratios 1.0, 1.5, and 2.0 with a complete end plate and with no end plate. The yawing axis for these examples is located at the tail apex. In order to illustrate the relative magnitudes of the two terms, the C_{n_β} contribution is also plotted in figure 20. It should be kept in mind in comparing the no-end-plate damping with the complete-end-plate damping that C_{n_r} is always greater (more negative) for a vertical tail with a complete end plate than with no end plate and that for any given aspect ratio C_{n_r} will decrease (become less negative) as the Mach number is increased. (Note that negative values of $C_{n_r} - C_{n_\beta}$ indicate positive damping.)

For the $A_v = 1.0$ tail shown in figure 20(a), the total damping of the complete-end-plate vertical tail is greater than that of the no-end-plate vertical tail. This occurs even though the $(-C_{n_\beta})$ contribution for the complete-end-plate tail is positive and therefore detracts from the total damping, $C_{n_r} + (-C_{n_\beta})$; whereas the $(-C_{n_\beta})$ contribution of the zero-end-plate $A_v = 1.0$ tail is slightly negative over the Mach number range for which the theory is valid and hence adds to the damping. As the aspect ratio is increased from 1.0 to 1.5 (fig. 20(b)), the damping of the complete-end-plate vertical tail decreases at a more rapid rate than the damping of the no-end-plate tail to the extent that the total damping for the complete-end-plate $A_v = 1.5$ vertical tail is now slightly less than the no-end-plate tail. This change may be attributed to the fact that the $(-C_{n_\beta})$ contribution to the

complete-end-plate tail damping increases more rapidly (becoming more positive) than the $(-C_{n\beta})$ component of the no-end-plate tail. Figure 20(c)

for the $A_v = 2.0$ vertical tail shows that the damping of the complete-end-plate vertical tail continues to decrease more rapidly than for the no-end-plate vertical tail so that the complete-end-plate tail damping becomes considerably less than that of the no-end-plate tail.

The damping derivatives plotted in figure 20, as pointed out, are for an axis location at the tail apex. In order to depict the effect of moving the yawing axis forward from this point, damping derivatives have been computed for the aspect-ratio-1.5 tail with a yawing axis located 1 chord ahead of the tail apex (fig. 21). These computations have been made with the aid of the transfer formulas in table V. A comparison of figures 20(b) and 21 shows that the damping qualities of the complete-end-plate vertical tail relative to the zero-end-plate vertical tail were considerably improved by moving the yawing axis forward. This improvement can be accounted for by the appearance of the β derivatives in the transfer formula for C_{n_r} .

CONCLUDING REMARKS

Pressure-distribution expressions and stability derivatives have been derived for zero-end-plate triangular vertical tails performing yawing, rolling, and constant-lateral-acceleration motions by a method for solving supersonic-conical-flow boundary-value problems. In addition, by using the yawing and constant-lateral-acceleration results, the damping of a vertical tail oscillating laterally in yaw has been approximated to the first order in frequency. End-plate effects have been discussed and suggestions made to aid in their evaluation. In this connection the complete-end-plate and no-end-plate stability derivatives for the sideslip motion obtained from other sources have been considered.

The pressure-distribution expressions and stability derivatives contained in this report are valid for a range of Mach numbers for which the leading edge is subsonic and the trailing edge supersonic.

Langley Aeronautical Laboratory,
National Advisory Committee for Aeronautics,
Langley Field, Va., August 10, 1954.

APPENDIX A

DEVELOPMENT OF EQUATIONS RELATING THE v-VELOCITY TO THE DISTRIBUTION
FUNCTION $f(\sigma)$ IN THE $y = 0$ PLANE

Equation (8) gives the expression for the velocity potential everywhere in space resulting from a distribution of doublets in the xz -plane with the strength of each doublet in this distribution being governed by the doublet-strength function $A(x, z)$. The derivative of this velocity potential with respect to any one of the coordinates x , y , or z will give the perturbation velocity in that direction. Of primary interest herein is the v -velocity, or the y -derivative of this potential, that is,

$$v(x, y, z) = \frac{\partial \phi_D(x, y, z)}{\partial y} \quad (A1)$$

for points on the xz -plane. Brown and Adams in reference 13 have constructed the velocity potential in space of a distribution of doublets by use of the following procedure. First, by using equations (8) and (18), the potential of a line of doublets in the xz -plane at an angle $\tan^{-1}\sigma$ to the x -axis is determined. This potential is given by

$$\phi = -\frac{B^2 y (x - B^2 \sigma z)}{(1 - B^2 \sigma^2)^{5/2}} \left(3 \coth^{-1} \gamma - \frac{\gamma}{\gamma^2 - 1} \right) + \frac{2B^2 y \sqrt{x^2 - B^2(y^2 + z^2)}}{(1 - B^2 \sigma^2)^2} \quad (A2)$$

where

$$\gamma = \frac{x - B^2 \sigma z}{\sqrt{1 - B^2 \sigma^2} \sqrt{x^2 - B^2(y^2 + z^2)}}$$

The velocity potential of a distribution of line doublets in the xz -plane, on the vertical tail, with strengths governed by the distribution function $f(\sigma)$ may then be written as

$$\phi = \int_0^C f(\sigma) \phi_L d\sigma \quad (A3)$$

where $\tan^{-1} C = \epsilon$, the apex angle of the vertical tail.

Substituting equation (A2) into equation (A3) and differentiating with respect to y yields the following equation for the v -velocity as $\beta y/x$ approaches zero:

$$\frac{v}{x} = \lim_{\eta \rightarrow 0} \left\{ \int_0^{B(\theta-\eta)} \left[\frac{Bf(\sigma)\sqrt{1-B^2\theta^2}(1-B^2\sigma\theta)^2}{(1-B^2\sigma^2)^2(B\sigma-B\theta)^2} - \frac{3Bf(\sigma)(1-B^2\sigma\theta)\coth^{-1}\xi}{(1-B^2\sigma^2)^{5/2}} \right. \right. +$$

$$\frac{2Bf(\sigma)\sqrt{1-B^2\theta^2}}{(1-B^2\sigma^2)^2} d(B\sigma) + \int_{B(\theta+\eta)}^{BC} \left[\frac{Bf(\sigma)\sqrt{1-B^2\theta^2}(1-B^2\sigma\theta)^2}{(1-B^2\sigma^2)^2(B\sigma-B\theta)^2} - \right.$$

$$\left. \left. \frac{3Bf(\sigma)(1-B^2\sigma\theta)\coth^{-1}\xi}{(1-B^2\sigma^2)^{5/2}} + \frac{2Bf(\sigma)\sqrt{1-B^2\theta^2}}{(1-B^2\sigma^2)^2} d(B\sigma) - \frac{2f(\theta)\sqrt{1-B^2\theta^2}}{\eta} \right] \right\} \quad (A4)$$

The singularity which occurs in the $\frac{\gamma}{y^2 - 1}$ term of equation (A2) when y is set equal to zero has been accounted for in equation (A4) (see ref. 13).

By taking the first and second derivatives of equation (A4) with respect to θ , two other useful relations are obtained. They are given in the appendix of reference 13 as

$$\frac{\partial(v/x)}{\partial\theta} = \lim_{\eta \rightarrow 0} \left\{ \int_0^{B(\theta-\eta)} \left[\frac{3B^3\sigma f(\sigma)\coth^{-1}\xi}{(1-B^2\sigma^2)^{5/2}} - \frac{B^2(3B\sigma+2B\theta+B\theta B^2\sigma^2)f(\sigma)}{\sqrt{1-B^2\theta^2}(1-B^2\sigma^2)^2} + \frac{B\theta B^2f(\sigma)}{\sqrt{1-B^2\theta^2}(B\sigma-B\theta)^2} - \right. \right. +$$

$$\frac{B^2f(\sigma)}{\sqrt{1-B^2\theta^2}(1-B^2\sigma^2)(B\sigma-B\theta)} + \frac{2B^2f(\sigma)\sqrt{1-B^2\theta^2}}{(B\sigma-B\theta)^3} d(B\sigma) + \int_{B(\theta+\eta)}^{BC} \left[\frac{3B^3\sigma f(\sigma)\coth^{-1}\xi}{(1-B^2\sigma^2)^{5/2}} - \right.$$

$$\frac{B^2(3B\sigma+2B\theta+B\theta B^2\sigma^2)f(\sigma)}{\sqrt{1-B^2\theta^2}(1-B^2\sigma^2)^2} + \frac{B\theta B^2f(\sigma)}{\sqrt{1-B^2\theta^2}(B\sigma-B\theta)^2} - \frac{B^2f(\sigma)}{\sqrt{1-B^2\theta^2}(1-B^2\sigma^2)(B\sigma-B\theta)} +$$

$$\left. \left. \frac{2B^2f(\sigma)\sqrt{1-B^2\theta^2}}{(B\sigma-B\theta)^3} d(B\sigma) - \frac{2B^2\theta f(\theta)}{\eta\sqrt{1-B^2\theta^2}} - \frac{4\sqrt{1-B^2\theta^2}f'(\theta)}{\eta} \right] \right\} \quad (A5)$$

and

$$\frac{\partial^2(v/x)}{\partial\theta^2} = \lim_{\eta \rightarrow 0} \left\{ 6\sqrt{1 - B^2\theta^2} \int_0^{B(\theta-\eta)} \frac{B^3 f(\sigma)}{(B\sigma - B\theta)^4} d(B\sigma) + \right.$$

$$6\sqrt{1 - B^2\theta^2} \int_{B(\theta+\eta)}^{BC} \frac{B^3 f(\sigma)}{(B\sigma - B\theta)^4} d(B\sigma) -$$

$$\left. \sqrt{1 - B^2\theta^2} \left[\frac{6f''(\theta)}{\eta} + \frac{4f(\theta)}{\eta^3} \right] \right\} \quad (A6)$$

The factor multiplying the $f''(\theta)$ term of the expression for $\frac{\partial^2(v/x)}{\partial\theta^2}$ as it appears in reference 13 is slightly in error and has been corrected in equation (A6).

Considering equations (5) and (7), it is evident that equation (A6) must be zero for both the rolling and yawing cases. This equation has already been satisfied by $f(\theta)$ (eq. (17)), since equation (A6) is in essence the integral equation which was inverted to obtain the general pressure expression from which $f(\theta)$ was derived (see ref. 15).

APPENDIX B

INTEGRATIONS TO OBTAIN v/x

The expression for v/x is, for θ approaching 0 (see eq. (19)),

$$\frac{v}{x} = \frac{1}{B} \int_0^{BC} \left[\frac{-3(MB\sigma + NBC)\sqrt{B\sigma(BC - B\sigma)} \tanh^{-1}\sqrt{1 - B^2\sigma^2}}{(1 - B^2\sigma^2)^{5/2}} + \right. \quad (1)$$

$$\left. \frac{2(MB\sigma + NBC)\sqrt{B\sigma(BC - B\sigma)}}{(1 - B^2\sigma^2)^2} d(B\sigma) + \right. \quad (2)$$

$$\left. \lim_{\theta \rightarrow 0} \left\{ \lim_{\eta \rightarrow 0} \left[\frac{1}{B} \int_0^{B(\theta-\eta)} \frac{(MB\sigma + NBC)\sqrt{B\sigma(BC - B\sigma)}(1 - B^2\sigma\theta)^2 \sqrt{1 - B^2\theta^2} d(B\sigma)}{(1 - B^2\sigma^2)^2 (B\sigma - B\theta)^2} + \right. \right. \right. \quad (3a)$$

$$\left. \left. \left. \frac{(MB\sigma + NBC)\sqrt{B\sigma(BC - B\sigma)}(1 - B^2\sigma\theta)^2 \sqrt{1 - B^2\theta^2} d(B\sigma)}{(1 - B^2\sigma^2)^2 (B\sigma - B\theta)^2} - \right] \right\} \quad (3b)$$

$$\left. \frac{2(MB\theta + NBC)\sqrt{B\theta(BC - B\theta)}\sqrt{1 - B^2\theta^2}}{B^2\eta} \right\} \quad (4)$$
(B1)

This expression has been broken into parts as indicated by the circled numbers with the third part being broken into two additional parts (3a) and (3b) because of the singularity in the integrand. Since (2) and (3) are elementary integrations similar to those found in most integral tables (see ref. 16), only (1) is dealt with in detail.

Performing the integrations (2) and (3) and combining the results yields

$$\frac{\sqrt{1 - B^2\theta^2}}{B} \left\{ \frac{2(MB\theta + \bar{N})\sqrt{B\theta(BC - B\theta)}}{B\eta} - \right.$$

$$\frac{\pi [M(-7B\theta BC - 2 + 10B\theta - BC) + \bar{N}(4 - 7BC + 4B\theta - B\theta BC)]}{8\sqrt{1 - BC}(1 - B\theta)} +$$

$$\left. \frac{\pi [M(-2 - 10B\theta + BC - 7B\theta BC) + \bar{N}(-4 + 4B\theta - 7BC + B\theta BC)]}{8\sqrt{1 + BC}(1 + B\theta)} \right\} \quad (B2)$$

where $\bar{N} = NBC$. The first term of expression (B2) exactly cancels (4), and the total of (2), (3), and (4) for $\theta \rightarrow 0$ is

$$\frac{\pi}{8B} \left[\frac{M(2 + BC) - \bar{N}(4 - 7BC)}{\sqrt{1 - BC}} + \frac{M(-2 + BC) - \bar{N}(4 + 7BC)}{\sqrt{1 + BC}} \right] \quad (B3)$$

The following two integrals comprising (1) remain to be evaluated:

$$\frac{-3}{B} \int_0^{BC} \frac{MB\sigma\sqrt{B\sigma(BC - B\sigma)} \tanh^{-1}\sqrt{1 - B^2\sigma^2} d(B\sigma)}{(1 - B^2\sigma^2)^{5/2}} \quad (B4)$$

$$\frac{-3}{B} \int_0^{BC} \frac{\bar{N}\sqrt{B\sigma(BC - B\sigma)} \tanh^{-1}\sqrt{1 - B^2\sigma^2} d(B\sigma)}{(1 - B^2\sigma^2)^{5/2}} \quad (B5)$$

It should be mentioned at this point that the integrands of expressions (B4) and (B5) are finite and continuous over the interval 0 to BC and therefore must yield a finite quantity when integrated.

The integration of expression (B4) by parts gives

$$\left[\frac{-M\sqrt{B\sigma(BC - B\sigma)} \tanh^{-1} \sqrt{1 - B^2\sigma^2}}{B(1 - B^2\sigma^2)^{3/2}} \right]_0^{BC} + \frac{M}{B} \int_0^{BC} \frac{(BC - 2B\sigma) \tanh^{-1} \sqrt{1 - B^2\sigma^2} d(B\sigma)}{2(1 - B^2\sigma^2)^{3/2} \sqrt{B\sigma(BC - B\sigma)}} - \\ \int_0^{BC} \frac{\sqrt{B\sigma(BC - B\sigma)} d(B\sigma)}{B\sigma(1 - B^2\sigma^2)^2} \quad (B6)$$

Integration of expression (B5) by parts gives

$$\left[\frac{-\bar{N}\sqrt{B\sigma(BC - B\sigma)} \tanh^{-1} \sqrt{1 - B^2\sigma^2}}{BB\sigma(1 - B^2\sigma^2)^{3/2}} \right]_0^{BC} - \int_0^{BC} \frac{\bar{N}BC \tanh^{-1} \sqrt{1 - B^2\sigma^2} d(B\sigma)}{2BB\sigma(1 - B^2\sigma^2)^{3/2} \sqrt{B\sigma(BC - B\sigma)}} - \\ \int_0^{BC} \frac{\bar{N}\sqrt{B\sigma(BC - B\sigma)} d(B\sigma)}{BB^2\sigma^2(1 - B^2\sigma^2)^2} \quad (B7)$$

Combining expressions (B6) and (B7) results in

$$\textcircled{1} = \left[\frac{-(MB\sigma + \bar{N})\sqrt{B\sigma(BC - B\sigma)} \tanh^{-1} \sqrt{1 - B^2\sigma^2}}{BB\sigma(1 - B^2\sigma^2)^{3/2}} \right]_0^{BC} - \\ \int_0^{BC} \frac{(MB\sigma + \bar{N})\sqrt{B\sigma(BC - B\sigma)} d(B\sigma)}{BB^2\sigma^2(1 - B^2\sigma^2)^2} + \\ \int_0^{BC} \frac{[MB\sigma(BC - 2B\sigma) - \bar{N}BC] \tanh^{-1} \sqrt{1 - B^2\sigma^2} d(B\sigma)}{2BB\sigma(1 - B^2\sigma^2)^{3/2} \sqrt{B\sigma(BC - B\sigma)}} \quad (B8)$$

The first term of equation (B8), when evaluated at the limits, is either zero or infinity. The integrand of $\textcircled{1}$ as was noted is finite over the

whole interval; therefore, infinities introduced as a result of parts integrations must, in the end, cancel themselves.

The second term of equation (B8) is an elementary integration which when evaluated (with infinities neglected) yields

$$\frac{\pi}{8B} \left(\frac{2M + 4\bar{N} - 3MBC - 5\bar{N}BC}{\sqrt{1 - BC}} - \frac{-4\bar{N} - 5\bar{N}BC + 2M + 3MBC}{\sqrt{1 + BC}} \right) \quad (B9)$$

It is now convenient in integrating the third term in equation (B8) to introduce the variable substitution

$$B\sigma = \frac{\zeta + k}{1 + k\zeta} \quad (B10)$$

so that BC and k are related by

$$BC = \frac{2k}{1 + k^2} \quad (B11)$$

The third term in equation (B8) when transformed by equation (B10) may be written in the form

$$\frac{-1}{B\sqrt{1 + k^2}(1 - k^2)} \sum_{i=1}^7 I_i \quad (B12)$$

where

$$I_1 = \int_{-k}^k \frac{M(1 + k^4)\zeta}{1 - \zeta^2} F(\zeta) d\zeta$$

$$I_2 = - \int_{-k}^k k(M + \bar{N}k^3)F(\zeta) d\zeta$$

$$I_3 = \int_{-k}^k \frac{Mk(1 + k^2) + 3\bar{N}k^2}{1 - \zeta^2} F(\zeta) d\zeta$$

$$I_4 = \int_{-k}^k \frac{\bar{N}k^4(k^2 - 2)}{k^2 - \zeta^2} F(\zeta) d\zeta$$

$$I_5 = \int_{-k}^k \frac{3\bar{N}k^3\zeta}{k^2 - \zeta^2} F(\zeta) d\zeta$$

$$I_6 = \int_{-k}^k \frac{\bar{N}k^2(1 - k^2)}{(1 - \zeta^2)(k^2 - \zeta^2)} F(\zeta) d\zeta$$

$$I_7 = - \int_{-k}^k \frac{\bar{N}k(1 - k^4\zeta^2)\zeta}{(1 - \zeta^2)(k^2 - \zeta^2)} F(\zeta) d\zeta$$

$$F(\zeta) = \frac{\tanh^{-1}\left(\frac{\sqrt{1-k^2}\sqrt{1-\zeta^2}}{1+k\zeta}\right)}{\sqrt{(1-\zeta^2)(k^2-\zeta^2)}}$$

The integrals I_1 , I_5 , and I_7 are elementary and may be determined by integration by parts. If the multiplicative factor before the summation sign in equation (B12) is neglected until all the components are totaled, these three components become

$$I_1 + I_5 + I_7 = \frac{-Mk(1 + k^4)\pi}{1 - k^2} - \frac{\bar{N}k^2(1 + k^2)\pi}{1 - k^2} \quad (B13)$$

Consider the integration required for I_2 , that is,

$$\int_{-k}^k \frac{\tanh^{-1}\left[\frac{\sqrt{(1-k^2)(1-\zeta^2)}}{1+k\zeta}\right] d\zeta}{\sqrt{(1-\zeta^2)(k^2-\zeta^2)}} \quad (B14)$$

Let $\zeta = k \sin \theta$; then expression (B14) becomes

$$\int_{-\pi/2}^{\pi/2} \frac{\tanh^{-1} \left[\frac{\sqrt{(1 - k^2)(1 - k^2 \sin^2 \theta)}}{1 + k^2 \sin \theta} \right] d\theta}{\sqrt{1 - k^2 \sin^2 \theta}} \quad (B15)$$

It can be shown that

$$\tanh^{-1} \left[\frac{\sqrt{(1 - k^2)(1 - k^2 \sin^2 \theta)}}{1 + k^2 \sin \theta} \right] = \tanh^{-1} \frac{\sqrt{1 - k^2}}{\sqrt{1 - k^2 \sin^2 \theta}} - \tanh^{-1} \frac{\sqrt{1 - k^2 \sin \theta}}{\sqrt{1 - k^2 \sin^2 \theta}} \quad (B16)$$

This fact allows expression (B15) to be rewritten as

$$\int_{-\pi/2}^{\pi/2} \frac{\tanh^{-1} \left(\frac{\sqrt{1 - k^2}}{\sqrt{1 - k^2 \sin^2 \theta}} \right) d\theta}{\sqrt{1 - k^2 \sin^2 \theta}} - \int_{-\pi/2}^{\pi/2} \frac{\tanh^{-1} \left(\frac{\sqrt{1 - k^2 \sin \theta}}{\sqrt{1 - k^2 \sin^2 \theta}} \right) d\theta}{\sqrt{1 - k^2 \sin^2 \theta}} \quad (B17)$$

The integrand of the second integral is an odd function; therefore, the integration between $-\pi/2$ and $\pi/2$ of this function is zero. Since the integrand of the first integral is an even function in θ , this integration may be expressed as

$$2 \int_0^{\pi/2} \frac{\tanh^{-1} \left(\frac{\sqrt{1 - k^2}}{\sqrt{1 - k^2 \sin^2 \theta}} \right) d\theta}{\sqrt{1 - k^2 \sin^2 \theta}} \quad (B18)$$

After the inverse hyperbolic tangent is replaced by its logarithmic equivalent and the additional variable transformation

$$\sin^2 \nu = \frac{1 - k^2}{1 - k^2 \sin^2 \theta} \quad (B19)$$

is introduced, expression (B18) becomes

$$\int_{\sin^{-1} \sqrt{1-k^2}}^{\pi/2} \log_e \frac{1 + \sin \nu}{1 - \sin \nu} \frac{d\nu}{\sqrt{\sin^2 \nu - (1 - k^2)}} \quad (B20)$$

It is convenient to let

$$\lambda = \sin^{-1} \sqrt{1 - k^2}$$

then

$$\sin^2 \lambda = 1 - k^2$$

Making these substitutions in expression (B20) gives

$$\int_{\lambda}^{\pi/2} \log_e \frac{1 + \sin \nu}{1 - \sin \nu} \frac{d\nu}{\sqrt{\sin^2 \nu - \sin^2 \lambda}} \quad (B21)$$

which is exactly in the form of the fourth integration formula of table 335 in reference 17. This formula gives the value of expression (B21) as $\pi K'(k)$. The integration of I_2 may now be expressed as

$$I_2 = -k(M + \bar{N}k^3)\pi K'(k) \quad (B22)$$

Using the same integrating procedure for I_3 , I_4 , and I_6 as just outlined for I_2 and the integration formulas in tables 335 and 336 of reference 17 leads to

$$I_3 = \frac{[Mk(1 + k^2) + 3\bar{N}k^2]\pi [1 + K'(k) - E'(k)]}{1 - k^2}$$

$$I_4 + I_6 = \pi \bar{N}(1 - k^2)k^2 \Pi \left\{ -(1-k^2), \sqrt{1-k^2}, \frac{\pi}{2} \right\} - \bar{N}(1 - k^2)k^2 \pi K'(k) -$$

$$\frac{\bar{N}k^2 \pi [1 + K'(k) - E'(k)]}{1 - k^2}$$

where $\Pi \left\{ -(1-k^2), \sqrt{1-k^2}, \frac{\pi}{2} \right\}$ is a complete elliptic integral of the third kind with modulus $\sqrt{1 - k^2}$ and parameter $-(1 - k^2)$.

Summing all the various parts contributing to the third term in equation (B8), including the common factor, gives the following expression:

$$\frac{-1}{B(1 - k^2)\sqrt{1 + k^2}} \left\{ \pi M k^3 + \pi \bar{N} k^2 + \frac{\pi K'(k) [2k^3 M + \bar{N} k^2 (1 + k^2)]}{1 - k^2} - \right.$$

$$\left. \frac{\pi E'(k) [2k^2 \bar{N} + M k (1 + k^2)]}{1 - k^2} + \bar{N} k^2 \pi (1 - k^2) \Pi \right\} \quad (B23)$$

The addition of expression (B23) to expression (B9) completely evaluates (1). Expression (B3) gives the evaluation of (2), (3), and (4). Before writing the total integration, the sum of expressions (B23), (B9), and (B3), it is desirable to combine expressions (B3) and (B9), which are functions of BC, and transform them by equation (B11) to functions of k. This procedure yields

$$\frac{\pi (\bar{N} k^2 + M k^3)}{B \sqrt{1 + k^2} (1 - k^2)} \quad (B24)$$

The total integration may now be written in terms of the parameter k as

$$\frac{-\pi}{B\sqrt{1+k^2(1-k^2)^2}} \left\{ K'(k) [2k^3M + \bar{N}k^2(1+k^2)] - E'(k) [2k^2\bar{N} + Mk(1+k^2)] + \bar{N}k^2(1-k^2)^2 \Pi \right\} \quad (B25)$$

By use of the process commonly known as interchanging the amplitude and parameter (see pp. 133 to 141 of ref. 21) the elliptic integral of the third kind appearing in equation (B25) is found to be equivalent to

$\frac{E'(k)}{k^2}$. This operation permits the expression for v/x (eq. (B25)) to assume the form given in equation (20) in the body of the report.

REFERENCES

1. Ribner, Herbert S.: The Stability Derivatives of Low-Aspect-Ratio Triangular Wings at Subsonic and Supersonic Speeds. NACA TN 1423, 1947.
2. Spreiter, John R.: The Aerodynamic Forces on Slender Plane- and Cruciform-Wing and Body Combinations. NACA Rep. 962, 1950. (Supersedes NACA TN's 1897 and 1662.)
3. Lomax, Harvard, and Heaslet, Max. A.: Damping-in-Roll Calculations for Slender Swept-Back Wings and Slender Wing-Body Combinations. NACA TN 1950, 1949.
4. Adams, Gaynor J.: Theoretical Damping in Roll and Rolling Effectiveness of Slender Cruciform Wings. NACA TN 2270, 1951.
5. Bobbitt, Percy J., and Malvestuto, Frank S., Jr.: Estimation of Forces and Moments Due to Rolling for Several Slender-Tail Configurations at Supersonic Speeds. NACA TN 2955, 1953.
6. Ribner, Herbert S.: Damping in Roll of Cruciform and Some Related Delta Wings at Supersonic Speeds. NACA TN 2285, 1951.
7. Martin, John C.: A Vector Study of Linearized Supersonic Flow Applications to Nonplanar Problems. NACA Rep. 1143, 1953. (Supersedes NACA TN 2641.)
8. Bleviss, Zigmund O.: Interference Effects in Supersonic Flow. Ph. D. Thesis, C.I.T., 1951.
9. Malvestuto, Frank S., Jr.: Theoretical Supersonic Force and Moment Coefficients on a Sideslipping Vertical- and Horizontal-Tail Combination With Subsonic Leading Edges and Supersonic Trailing Edges. NACA TN 3071, 1954.
10. Martin, John C., and Malvestuto, Frank S., Jr.: Theoretical Force and Moments Due to Sideslip of a Number of Vertical Tail Configurations at Supersonic Speeds. NACA TN 2412, 1951.
11. Heaslet, Max. A., Lomax, Harvard, and Jones, Arthur L.: Volterra's Solution of the Wave Equation as Applied to Three-Dimensional Supersonic Airfoil Problems. NACA Rep. 889, 1947. (Supersedes NACA TN 1412.)
12. Brown, Clinton E.: Theoretical Lift and Drag of Thin Triangular Wings at Supersonic Speeds. NACA Rep. 839, 1946. (Supersedes NACA TN 1183.)

13. Brown, Clinton E., and Adams, Mac C.: Damping in Pitch and Roll of Triangular Wings at Supersonic Speeds. NACA Rep. 892, 1948. (Supersedes NACA TN 1566.)
14. Busemann, Adolf: Infinitesimal Conical Supersonic Flow. NACA TM 1100, 1947.
15. Lomax, Harvard, and Heaslet, Max. A.: Generalized Conical-Flow Fields in Supersonic Wing Theory. NACA TN 2497, 1951.
16. Peirce, B. O.: A Short Table of Integrals. Third rev. ed., Ginn and Co., 1929.
17. De Haan, D. Bierens: Nouvelles Tables D'Intégrales Définies. G. E. Stechart & Co. (New York), 1939, pp. 475-476.
18. Ribner, Herbert S.: Time-Dependent Downwash at the Tail and the Pitching Moment Due to Normal Acceleration at Supersonic Speeds. NACA TN 2042, 1950.
19. Gardner, C.: Time-Dependent Linearized Supersonic Flow Past Planar Wings. Communications on Pure and Appl. Math., vol. III, no. 1, Mar. 1950, pp. 33-38.
20. Malvestuto, Frank S., Jr., and Margolis, Kenneth: Theoretical Stability Derivatives of Thin Sweptback Wings Tapered to a Point With Sweptback or Sweptforward Trailing Edges for a Limited Range of Supersonic Speeds. NACA Rep. 971, 1950. (Supersedes NACA TN 1761.)
21. Cayley, Arthur: An Elementary Treatise on Elliptic Functions. Second ed., George Bell and Sons, Ltd. (London), 1895.

TABLE I.- LATERAL STABILITY DERIVATIVES FOR ZERO-END-PLATE
TRIANGULAR VERTICAL TAILS

Derivative	Formula
$B(G_{Y_p})_0$	$\pi A_v B \sqrt{\frac{2BC}{A_v B}} \left(\frac{M_p'}{4} + \frac{N_p'}{4} + \frac{BCN_p'}{2A_v B} \right)$
$B(G_l)_0$	$\frac{\pi A_v B}{16} \sqrt{\frac{2BC}{A_v B}} \left(\frac{5M_p'}{2} + \frac{5N_p'}{2} + \frac{3BCN_p'}{A_v B} \right)$
$(C_{n_p})_0$	$-\pi A_v B \sqrt{\frac{2BC}{A_v B}} \left[M_p' \left(\frac{5}{32BC} + \frac{1}{16A_v B} \right) + N_p' \left(\frac{5}{32BC} + \frac{1}{4A_v B} + \frac{3BC}{8A_v^2 B^2} \right) \right]$
$(C_{Y_r})_0$	$\pi A_v B \sqrt{\frac{2BC}{A_v B}} \left(\frac{M_r'}{4} + \frac{N_r'}{4} + \frac{BCN_r'}{2A_v B} \right)$
$(C_l_r)_0$	$\frac{\pi A_v B}{16} \sqrt{\frac{2BC}{A_v B}} \left(\frac{5M_r'}{2} + \frac{5N_r'}{2} + \frac{3BCN_r'}{A_v B} \right)$
$(C_{n_r})_0/B$	$-\pi A_v B \sqrt{\frac{2BC}{A_v B}} \left[M_r' \left(\frac{5}{32BC} + \frac{1}{16A_v B} \right) + N_r' \left(\frac{5}{32BC} + \frac{1}{4A_v B} + \frac{3BC}{8A_v^2 B^2} \right) \right]$
$B(G_{Y_\beta})_0$	$\frac{-\pi \sqrt{A_v B} \sqrt{1 - \sqrt{1 - B^2 C^2}}}{E'(k) \sqrt{BC}}$
$B(G_l)_0$	$\frac{-\pi \sqrt{A_v B} \sqrt{1 - \sqrt{1 - B^2 C^2}}}{2E'(k) \sqrt{BC}}$
$(C_{n_\beta})_0$	$\frac{\pi \sqrt{BC} \sqrt{1 - \sqrt{1 - B^2 C^2}}}{3B^2 C^2 E'(k) \sqrt{A_v B}} \left(\frac{3A_v B}{2} + BC \right)$

TABLE I.- LATERAL STABILITY DERIVATIVES FOR ZERO-END-PLATE
TRIANGULAR VERTICAL TAILS - Concluded

Derivative	Formula
$(C_{Y\dot{\beta}})_0$	$-\frac{\pi A_v B}{A_v B} \sqrt{\frac{2BC}{A_v B}} \left[\frac{M_r'}{4} + \left(1 + \frac{2BC}{A_v B} \right) \frac{N_r'}{4} - \frac{\sqrt{2} \sqrt{1 - \sqrt{1 - B^2 C^2}}}{4B^2 C^2 E'(k)} - \right.$ $\left. \frac{\sqrt{2} \sqrt{1 - \sqrt{1 - B^2 C^2}}}{6BCA_v B E'(k)} - \frac{\pi A_v B}{B^2} \sqrt{\frac{2BC}{A_v B}} \left[\frac{M_r'}{4} + \left(1 + \frac{2BC}{A_v B} \right) \frac{N_r'}{4} - \right. \right.$ $\left. \left. \frac{\sqrt{2} \sqrt{1 - \sqrt{1 - B^2 C^2}}}{4B^2 C^2 E'(k)} - \frac{\sqrt{2} \sqrt{1 - \sqrt{1 - B^2 C^2}}}{2BCA_v B E'(k)} \right] \right]$
$(C_{n\dot{\beta}})_0$	$\frac{\pi A_v B}{A_v B} \sqrt{\frac{2BC}{A_v B}} \left\{ B \left[M_r' \left(\frac{5}{32BC} + \frac{1}{16A_v B} \right) + N_r' \left(\frac{5}{32BC} + \frac{1}{4A_v B} + \frac{5BC}{8A_v^2 B^2} \right) - \right. \right.$ $\left. \left. \frac{\sqrt{2} \sqrt{1 - \sqrt{1 - B^2 C^2}}}{E'(k)} \left(\frac{5}{32B^3 C^3} + \frac{1}{8B^2 C^2 A_v B} + \frac{1}{8BCA_v^2 B^2} \right) \right] + \right.$ $\left. \frac{1}{B} \left[M_r' \left(\frac{5}{32BC} + \frac{1}{16A_v B} \right) + N_r' \left(\frac{5}{32BC} + \frac{1}{4A_v B} + \frac{5BC}{8A_v^2 B^2} \right) - \right. \right.$ $\left. \left. \frac{\sqrt{2} \sqrt{1 - \sqrt{1 - B^2 C^2}}}{E'(k)} \left(\frac{5}{32B^3 C^3} + \frac{1}{4B^2 C^2 A_v B} + \frac{5}{8BCA_v^2 B^2} \right) \right] \right\}$
$(C_{l\dot{\beta}})_0$	$-\frac{\pi A_v B}{32} \sqrt{\frac{2BC}{A_v B}} \left[5M_r' + 5N_r' + \frac{6BCN_r'}{A_v B} - \right.$ $\left. \frac{\sqrt{2} \sqrt{1 - \sqrt{1 - B^2 C^2}}}{E'(k)} \left(\frac{5}{B^2 C^2} + \frac{2}{BCA_v B} \right) \right] -$ $\frac{\pi A_v B}{32B^2} \sqrt{\frac{2BC}{A_v B}} \left[5M_r' + 5N_r' + \frac{6BCN_r'}{A_v B} - \right.$ $\left. \left. \frac{\sqrt{2} \sqrt{1 - \sqrt{1 - B^2 C^2}}}{E'(k)} \left(\frac{5}{B^2 C^2} + \frac{6}{BCA_v B} \right) \right] \right]$

TABLE II.- LATERAL STABILITY DERIVATIVES FOR ZERO-END-PLATE
HALF-DELTA VERTICAL TAILS

Derivative	Formula
$B(C_{Y_P})_0$	$\frac{\pi BC}{2}(M_P' + 2N_P')$
$(C_{n_P})_0$	$-\pi \frac{3}{8}(M_P' + 2N_P')$
$B(C_{l_P})_0$	$\frac{\pi BC}{2} \left(\frac{5}{3} M_P' + N_P' \right)$
$(C_{Y_T})_0$	$\frac{\pi BC}{2}(M_T' + 2N_T')$
$(C_{n_T})_0$	$-\frac{3\pi B}{8}(M_T' + 2N_T')$
$(C_{l_T})_0$	$\frac{\pi BC}{2} \left(\frac{5}{3} M_T' + N_T' \right)$
$B(C_{Y_B})_0$	$\frac{-\pi}{E'(k)} \sqrt{2(1 - \sqrt{1 - B^2 C^2})}$
$(C_{n_B})_0$	$\frac{2\pi}{3BCE'(k)} \sqrt{2(1 - \sqrt{1 - B^2 C^2})}$
$B(C_{l_B})_0$	$\frac{-\pi}{2E'(k)} \sqrt{2(1 - \sqrt{1 - B^2 C^2})}$
$(C_{Y_B})_0$	$- \frac{BCx}{2} \left[M_T' + 2N_T' - 4 \frac{\sqrt{2(1 - \sqrt{1 - B^2 C^2})}}{3B^2 C^2 E'(k)} \right] -$ $\frac{BCx}{2B^2} \left[M_T' + 2N_T' - 2 \frac{\sqrt{2(1 - \sqrt{1 - B^2 C^2})}}{B^2 C^2 E'(k)} \right]$
$(C_{n_B})_0$	$\frac{\pi B}{4} \left[\frac{3}{2} M_T' + 3N_T' - 2 \frac{\sqrt{2(1 - \sqrt{1 - B^2 C^2})}}{B^2 C^2 E'(k)} \right] +$ $\frac{\pi}{4B} \left[\frac{3}{2} M_T' + 3N_T' - 3 \frac{\sqrt{2(1 - \sqrt{1 - B^2 C^2})}}{B^2 C^2 E'(k)} \right]$
$(C_{l_B})_0$	$\frac{-BCx}{4} \left[2N_T' + \frac{5}{4} M_T' - 3 \frac{\sqrt{2(1 - \sqrt{1 - B^2 C^2})}}{2B^2 C^2 E'(k)} \right] -$ $\frac{BCx}{4B^2} \left[2N_T' + \frac{5}{4} M_T' - 2 \frac{\sqrt{2(1 - \sqrt{1 - B^2 C^2})}}{B^2 C^2 E'(k)} \right]$

TABLE III.- LATERAL STABILITY DERIVATIVES FOR COMPLETE-END-PLATE

TRIANGULAR VERTICAL TAILS

[Formulas obtained from reference 20]

Derivative	Formula
$B(C_{Y_B})_C$	$\frac{-2BA_v(1-R)^{1/2}}{E'(BC)(1+R)^{3/2}} \left(\frac{\pi}{2} + \sin^{-1}R + R\sqrt{1-R^2} \right)$
$(C_{n_B})_C$	$\frac{4(1-R)^2}{3E'(BC)(1-R^2)^{5/2}} \left[(2+R^2) \left(\frac{\pi}{2} + \sin^{-1}R \right) + R(4-R^2)\sqrt{1-R^2} \right]$
$(C_{Y_R})_C$	$\frac{4G(BC)(1-R)^2}{3(1-R^2)^{5/2}} \left[3 \left(\frac{\pi}{2} + \sin^{-1}R \right) + R(5-2R^2)\sqrt{1-R^2} \right]$
$(C_{n_R})_C$	$\frac{-BG(BC)(1-R)^3}{3BC(1-R^2)^{7/2}} \left[3(2R^2+3) \left(\frac{\pi}{2} + \sin^{-1}R \right) + R(4R^4 - 12R^2 + 23)\sqrt{1-R^2} \right]$
$(C_{Y_B})_C$	$\frac{4(1-R)^2}{3(1-R^2)^{5/2}} \left\{ \frac{[1-E'(BC)G(BC)]}{B^2E'(BC)} \left[3 \left(\frac{\pi}{2} + \sin^{-1}R \right) + R(5-2R^2)\sqrt{1-R^2} \right] - G(BC) \left[3 \left(\frac{\pi}{2} + \sin^{-1}R \right) + R(5-2R^2)\sqrt{1-R^2} \right] + \frac{1}{E'(BC)} \left[(2+R^2) \left(\frac{\pi}{2} + \sin^{-1}R \right) + R(4-R^2)\sqrt{1-R^2} \right] \right\}$
$(C_{n_B})_C$	$\frac{-(1-R)^3}{3(1-R^2)^{7/2}BC} \left(\frac{[1-E'(BC)G(BC)]}{E'(BC)} \left[3(2R^2+3) \left(\frac{\pi}{2} + \sin^{-1}R \right) + R(4R^4 - 12R^2 + 23)\sqrt{1-R^2} \right] + B \left\{ 3 \left(\frac{\pi}{2} + \sin^{-1}R \right) \left[\frac{3R^2+2}{E'(BC)} - G(BC)(2R^2+3) \right] + R\sqrt{1-R^2} \left[\frac{2R^4-5R^2+18}{E'(BC)} - G(BC)(4R^4 - 12R^2 + 23) \right] \right\} \right)$

TABLE IV.- LATERAL STABILITY DERIVATIVES FOR COMPLETE-END-PLATE
HALF-DELTA VERTICAL TAILS*

$$\left[G(BC) = \frac{1 - B^2 C^2}{(1 - 2B^2 C^2)E'(BC) + B^2 C^2 K'(BC)} \right]$$

Derivative	Formula
$B(C_{Y\beta})_C$	$\frac{-2\pi BC}{E'(BC)}$
$(C_{n\beta})_C$	$\frac{4\pi}{3E'(BC)}$
$(C_{Yr})_C$	$2\pi G(BC)$
$(C_{nr})_C$	$\frac{-3\pi BG(BC)}{2BC}$
$(C_{Y\dot{\beta}})_C$	$\frac{2\pi}{B^2} \left[-G(BC) + \frac{1}{E'(BC)} \right] + 2\pi \left[-G(BC) + \frac{2}{3E'(BC)} \right]$
$(C_{n\dot{\beta}})_C$	$\frac{-3\pi}{2BBC} \left[-G(BC) + \frac{1}{E'(BC)} \right] - \frac{3\pi B}{2BC} \left[-G(BC) + \frac{2}{3E'(BC)} \right]$

* $(C_l\beta)_C$ can be obtained from reference 9.

TABLE V.- TRANSFER FORMULAS

Stability derivatives in a body system of axes with origin at tail apex	Formulas for transfer to a body system of axes with origin displaced distances x_0 (positive forward) and z_0 (positive downward) from tail apex
$C_{Y\beta}$	$C_{Y\beta}$
$C_{n\beta}$	$C_{n\beta} - \frac{x_0}{b_v} C_{Y\beta}$
$C_{l\beta}$	$C_{l\beta} + \frac{z_0}{b_v} C_{Y\beta}$
C_{Y_p}	C_{Y_p}
C_{n_p}	$C_{n_p} - \frac{x_0}{b_v} C_{Y_p}$
C_{l_p}	$C_{l_p} + \frac{z_0}{b_v} C_{Y_p}$
C_{Y_r}	$C_{Y_r} - \frac{x_0}{b_v} C_{Y\beta}$
C_{n_r}	$C_{n_r} - \frac{x_0}{b_v} (C_{n\beta} + C_{Y_r}) + \left(\frac{x_0}{b_v}\right)^2 C_{Y\beta}$
C_{l_r}	$C_{l_r} + \frac{z_0}{b_v} C_{Y_r} - \frac{x_0}{b_v} C_{l\beta} - \frac{z_0}{b_v} \frac{x_0}{b_v} C_{Y\beta}$
$C_{Y\dot{\beta}}$	$C_{Y\dot{\beta}}$
$C_{n\dot{\beta}}$	$C_{n\dot{\beta}} - \frac{x_0}{b_v} C_{Y\dot{\beta}}$
$C_{l\dot{\beta}}$	$C_{l\dot{\beta}} + \frac{z_0}{b_v} C_{Y\dot{\beta}}$

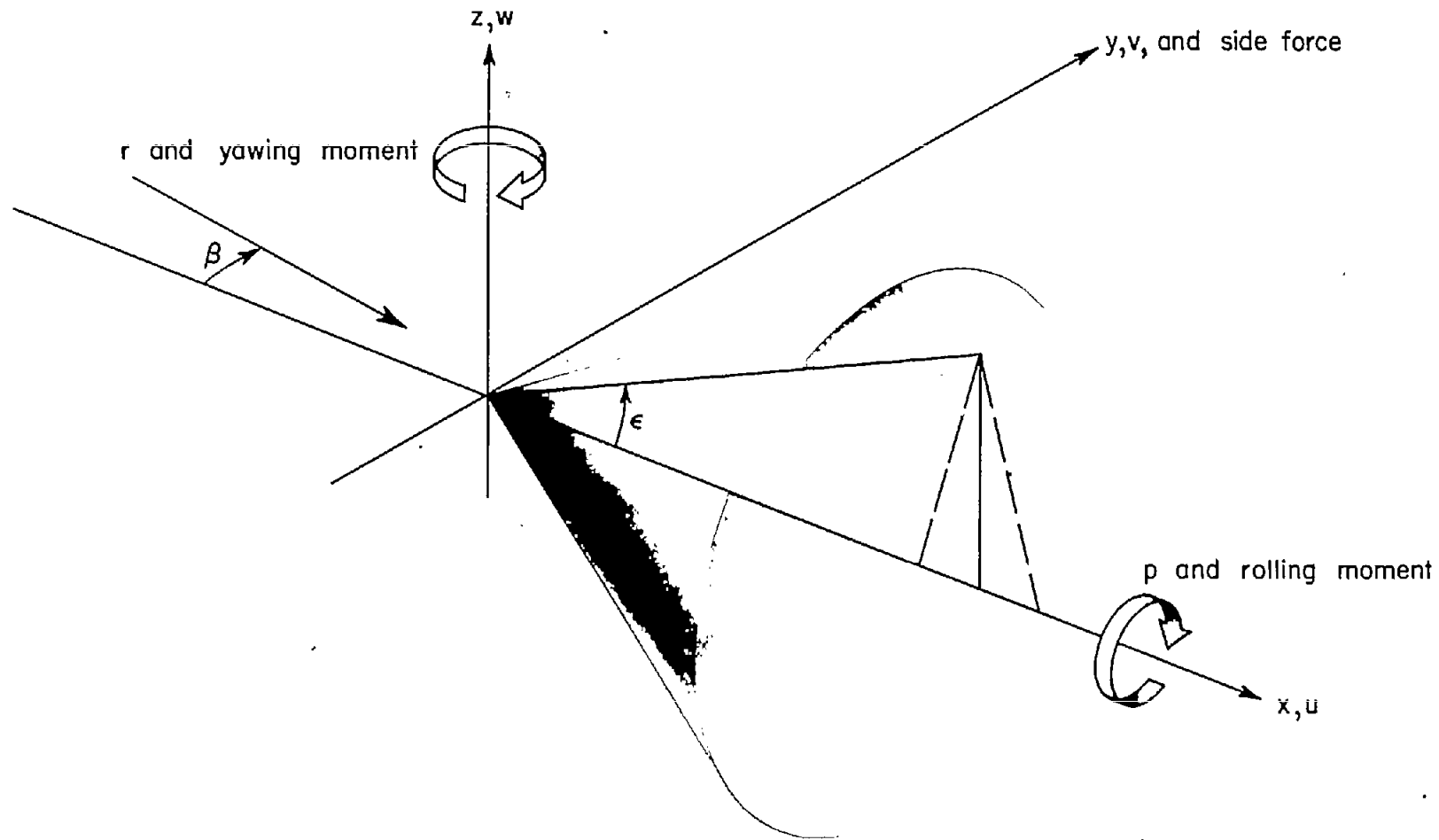


Figure 1.- Sketch of the vertical tail showing the axes system used in L-85624 the analysis and the positive directions of the forces, moments, velocities, and angles. Dashed lines on vertical tail indicate that the trailing edge may be swept forward or backward.

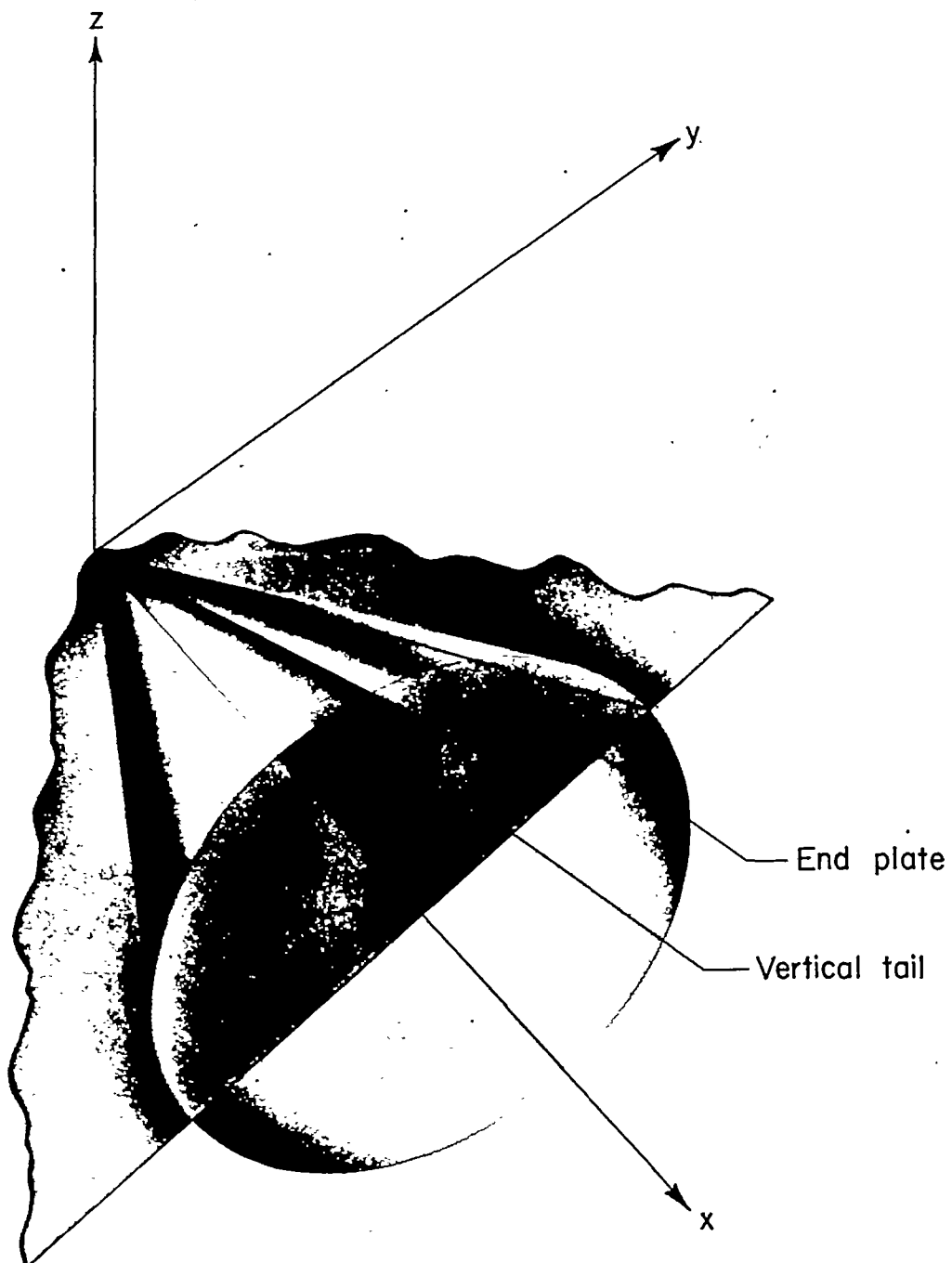
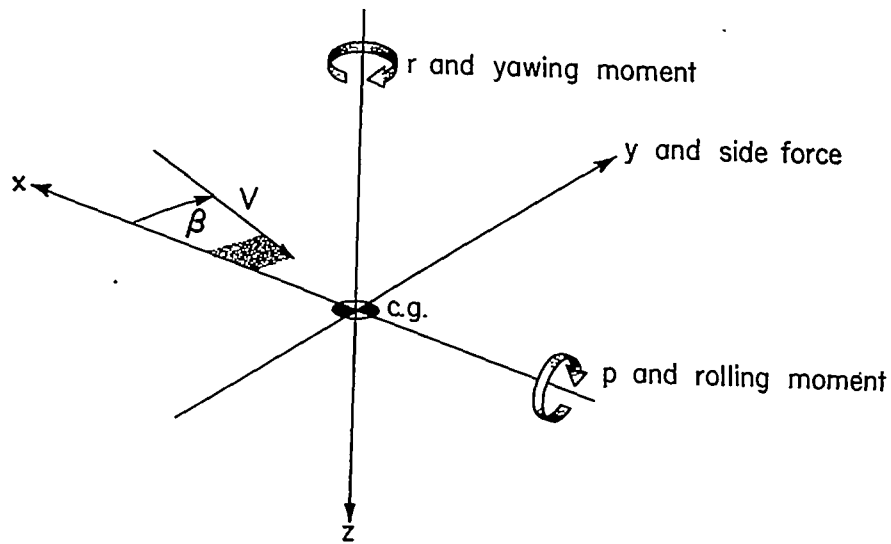
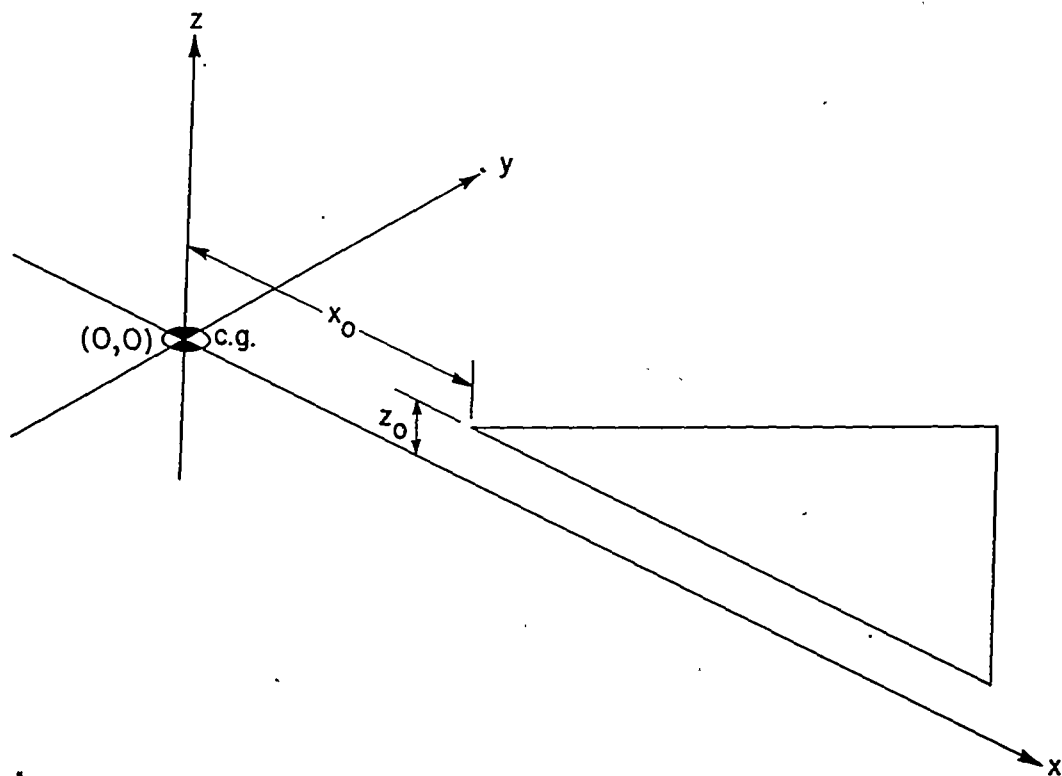


Figure 2.- Half-delta tail mounted on a complete end plate. L-85625



(a) Positive direction of forces and moments in the stability axes system ($\alpha = 0^\circ$).



(b) Axes system to which force and moment derivatives may be transferred by use of table V.

Figure 3.- Systems of axes.

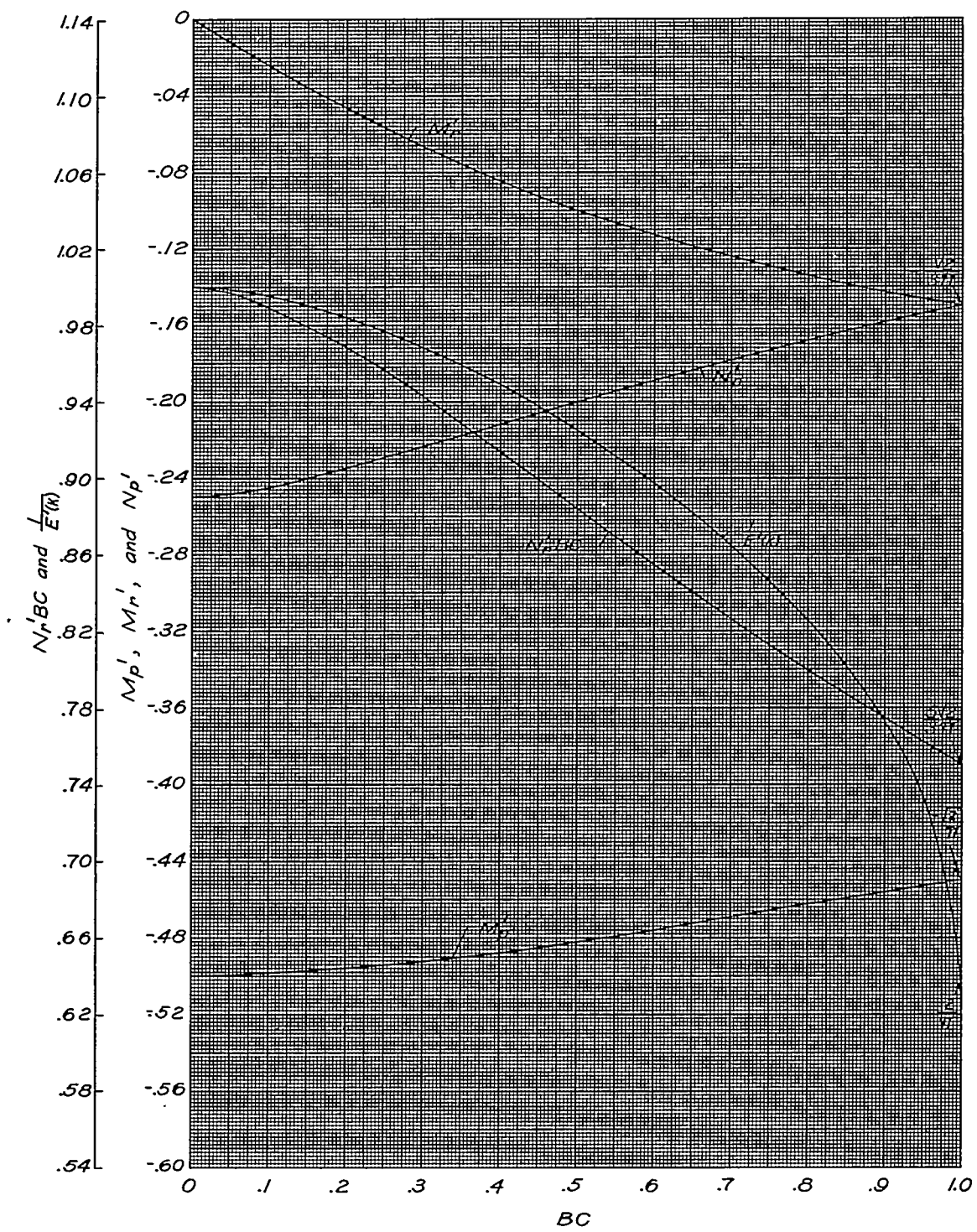


Figure 4.- Variation of the parameters $N_r'BC$, M_r' , N_p' , M_p' , and $1/E'(k)$ with BC . These curves are of use in computing the no-end-plate stability derivatives given in tables I and II.

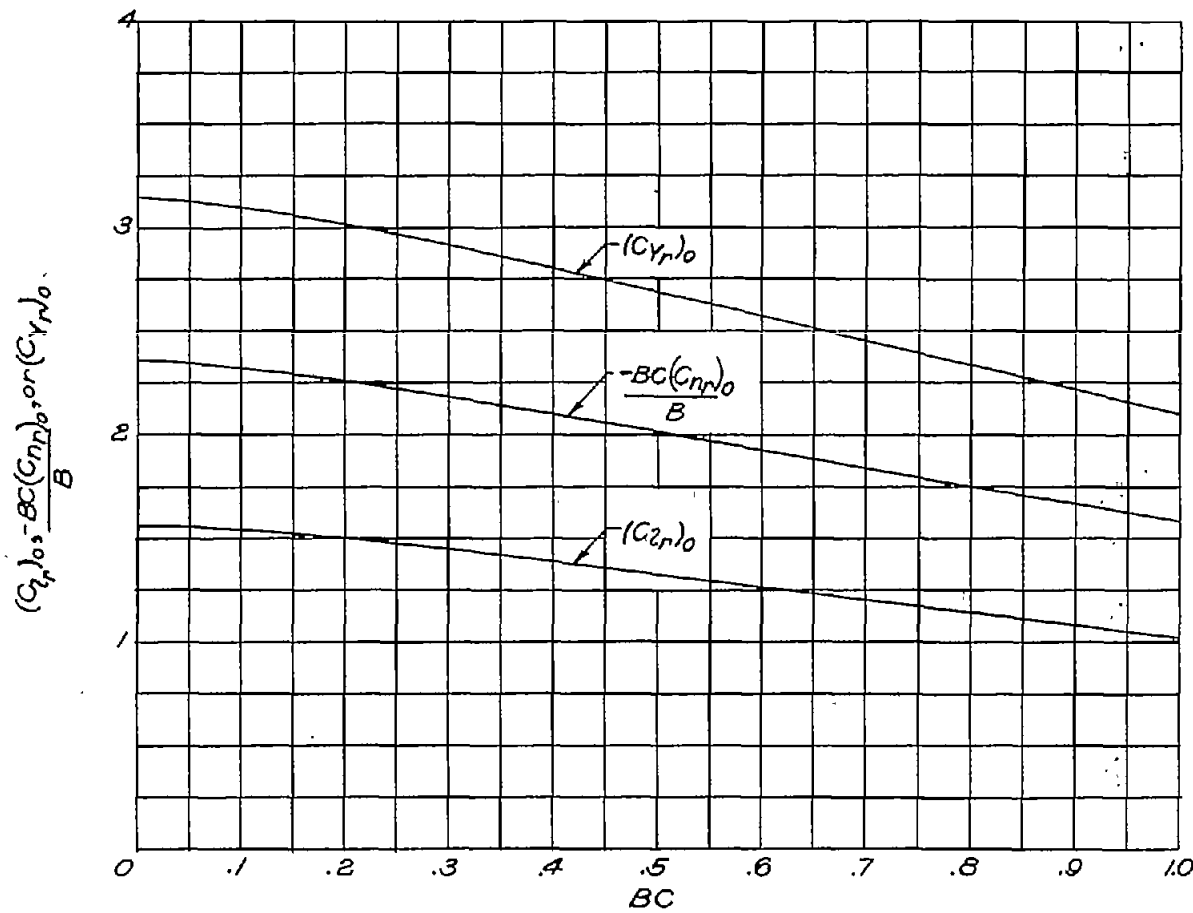


Figure 5.- Variation of the zero-end-plate half-delta vertical-tail stability derivatives $(C_{Yr})_0$ and $(C_{lr})_0$ and the stability-derivative parameter $\frac{-BC(C_{nr})_0}{B}$ with the leading-edge sweep parameter BC .

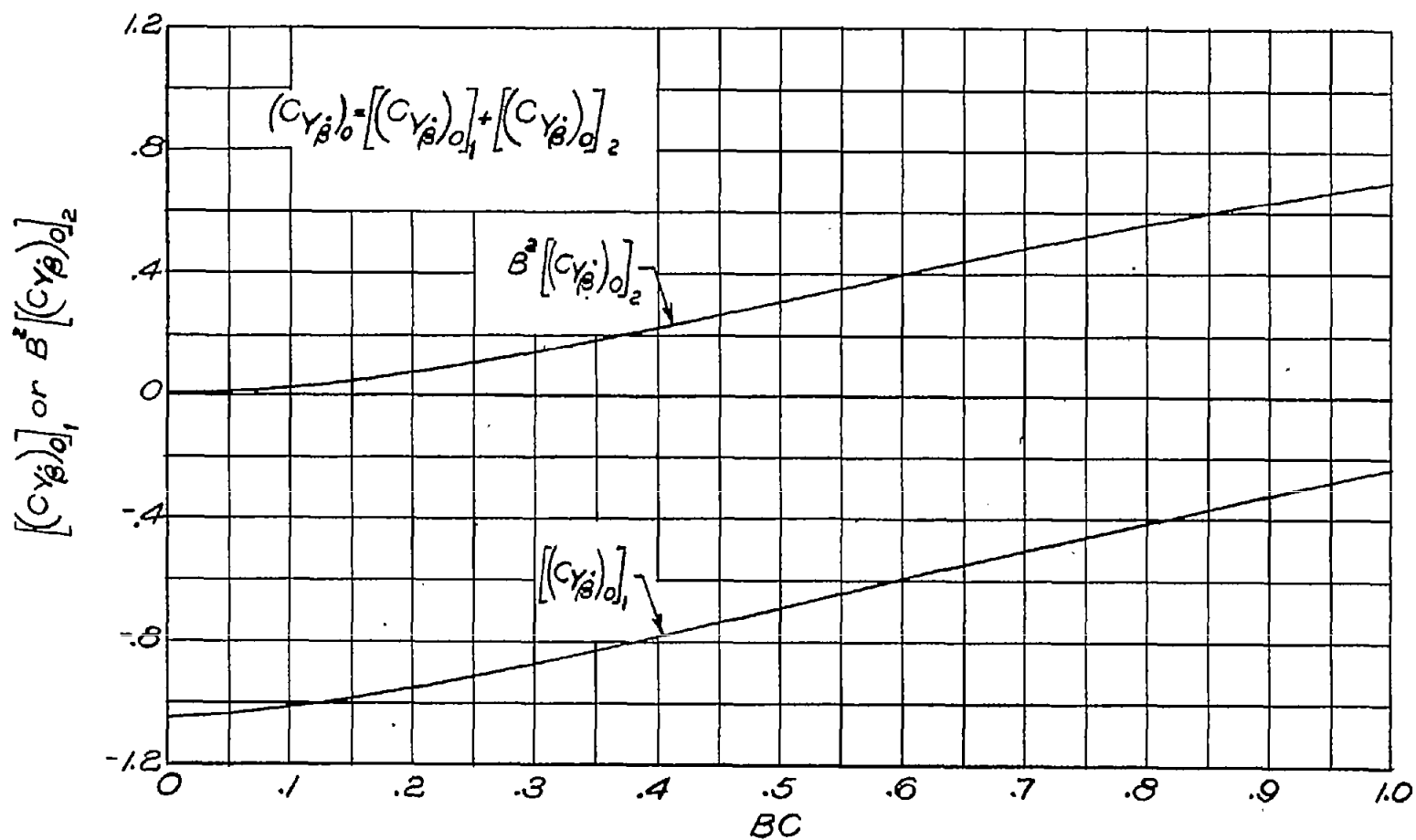


Figure 6.- Variation with BC of the quantities $[C_{Y\beta}]_0]_1$ and $B^2 [C_{Y\beta}]_0]_2$ for the half-delta tail. Note that the stability derivative $(C_{Y\beta})_0$ is given by the sum of $[C_{Y\beta}]_0]_1$ and $[C_{Y\beta}]_0]_2$.

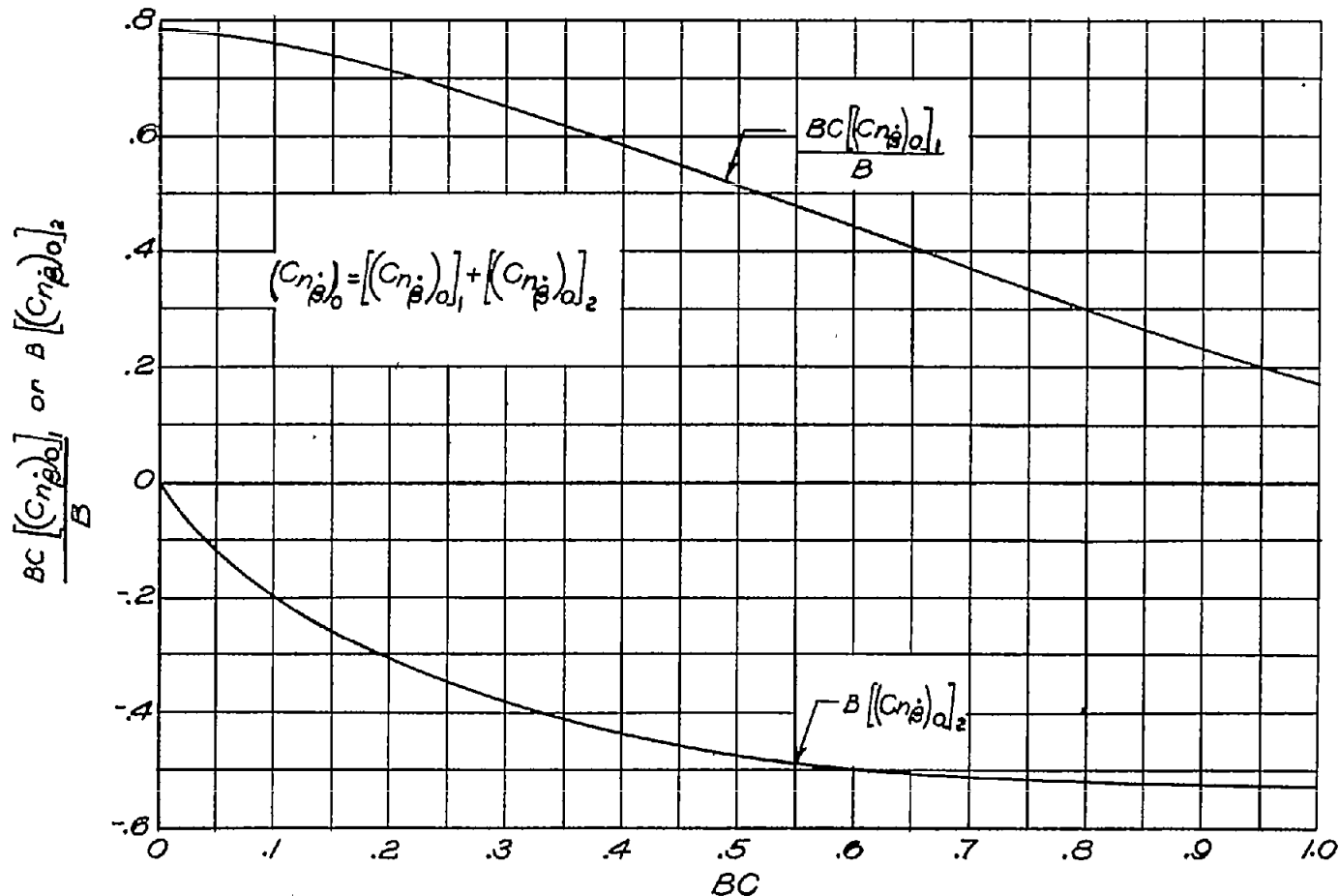


Figure 7.- Variation with BC of the quantities $\frac{BC[(C_{n\beta})_0]_1}{B}$ and $B[(C_{n\beta})_0]_2$ for the half-delta tail. Note that the stability derivative $(C_{n\beta})_0$ is given by the sum of $[(C_{n\beta})_0]_1$ and $[(C_{n\beta})_0]_2$.

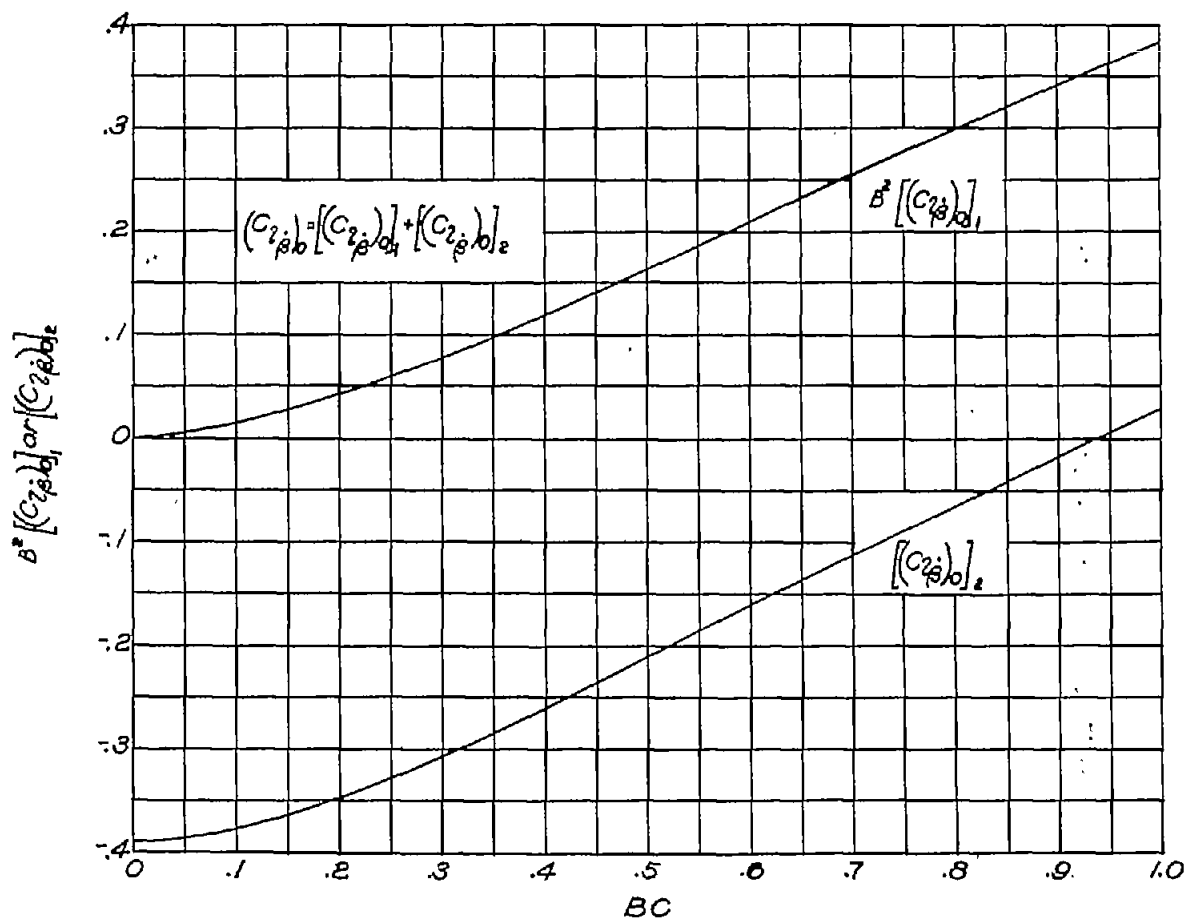


Figure 8.- Variation with BC of the quantities $B^2 \left[\begin{matrix} C_l \\ \beta \end{matrix} \right]_0 \left[\begin{matrix} C_r \\ \beta \end{matrix} \right]_0$ and $\left[\begin{matrix} C_l \\ \beta \end{matrix} \right]_0 \left[\begin{matrix} C_r \\ \beta \end{matrix} \right]_0$ for the half-delta tail. Note that the stability derivative $\left[\begin{matrix} C_l \\ \beta \end{matrix} \right]_0$ is given by the sum of $\left[\begin{matrix} C_l \\ \beta \end{matrix} \right]_0 \left[\begin{matrix} C_r \\ \beta \end{matrix} \right]_1$ and $\left[\begin{matrix} C_l \\ \beta \end{matrix} \right]_0 \left[\begin{matrix} C_r \\ \beta \end{matrix} \right]_2$.

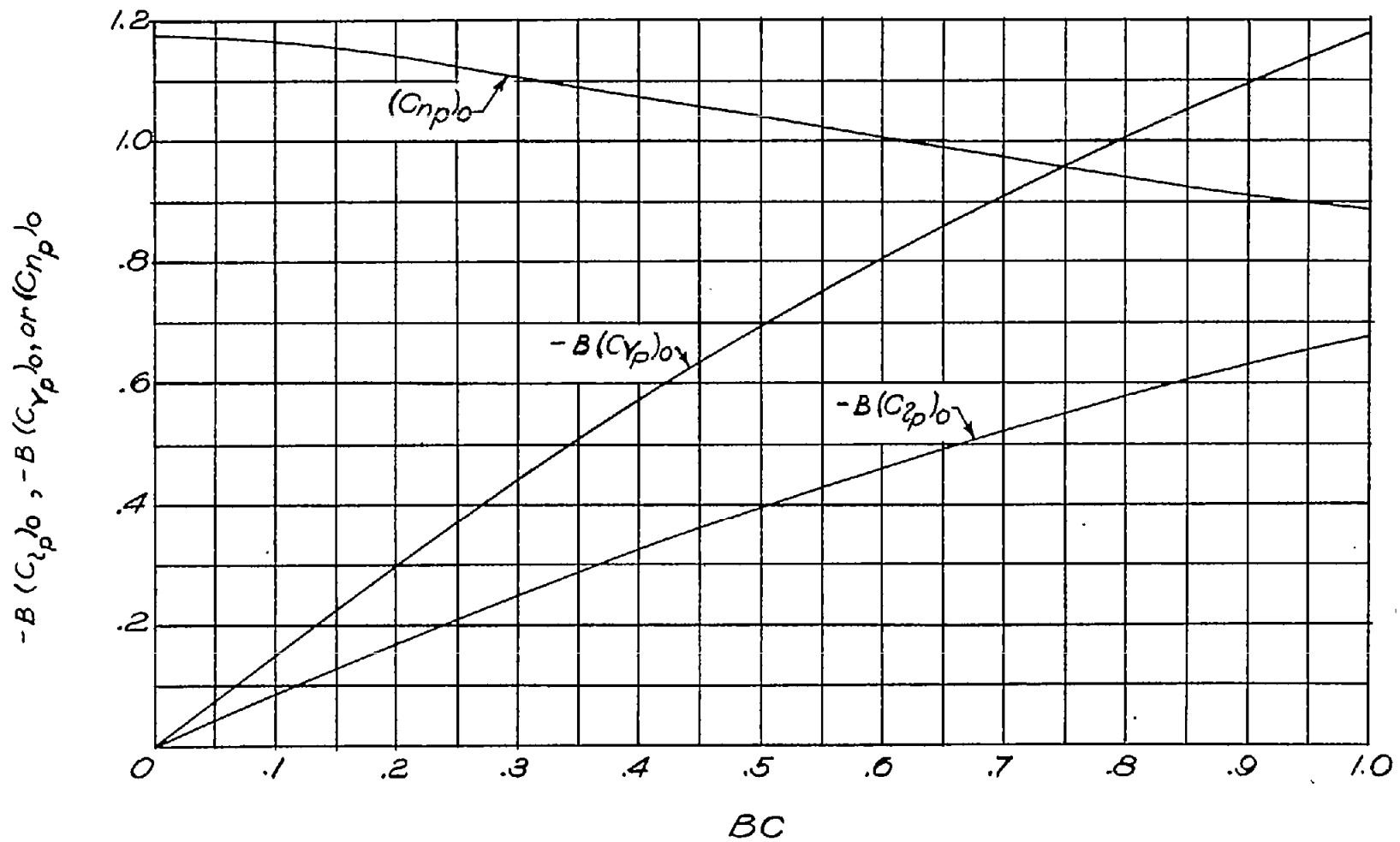


Figure 9.- The variation of $-B(C_{l_p})_0$, $-B(C_{Y_p})_0$, and $(C_{n_p})_0$ with BC for the half-delta tail.

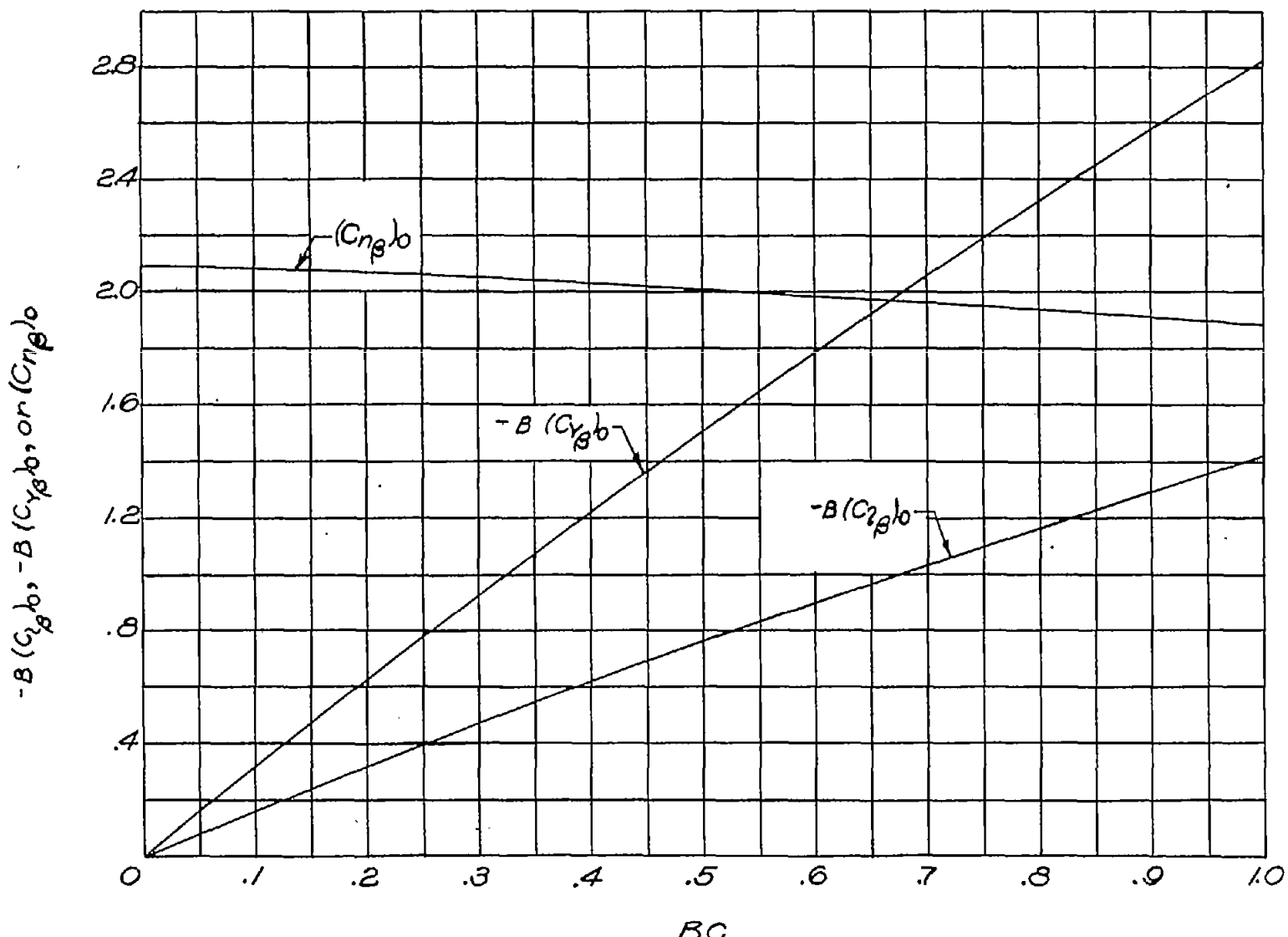


Figure 10.- The variation of $-B(C_{i\beta})_0$, $-B(C_{Y\beta})_0$, and $(C_{n\beta})_0$ with BC for the half-delta tail.

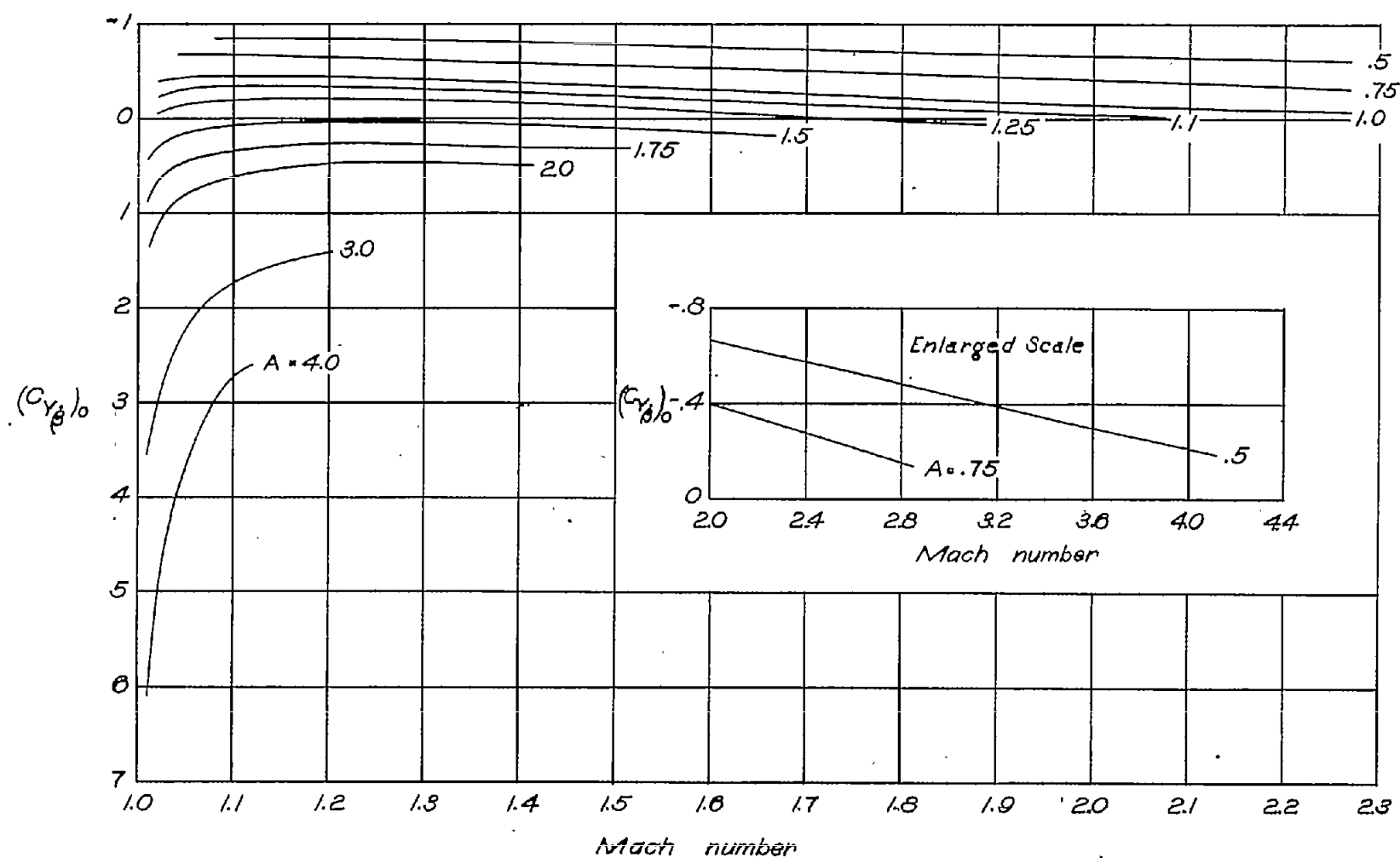


Figure 11.- The variation of $(C_{Y_B})_0$ with Mach number for a number of aspect ratios of a half-delta tail.

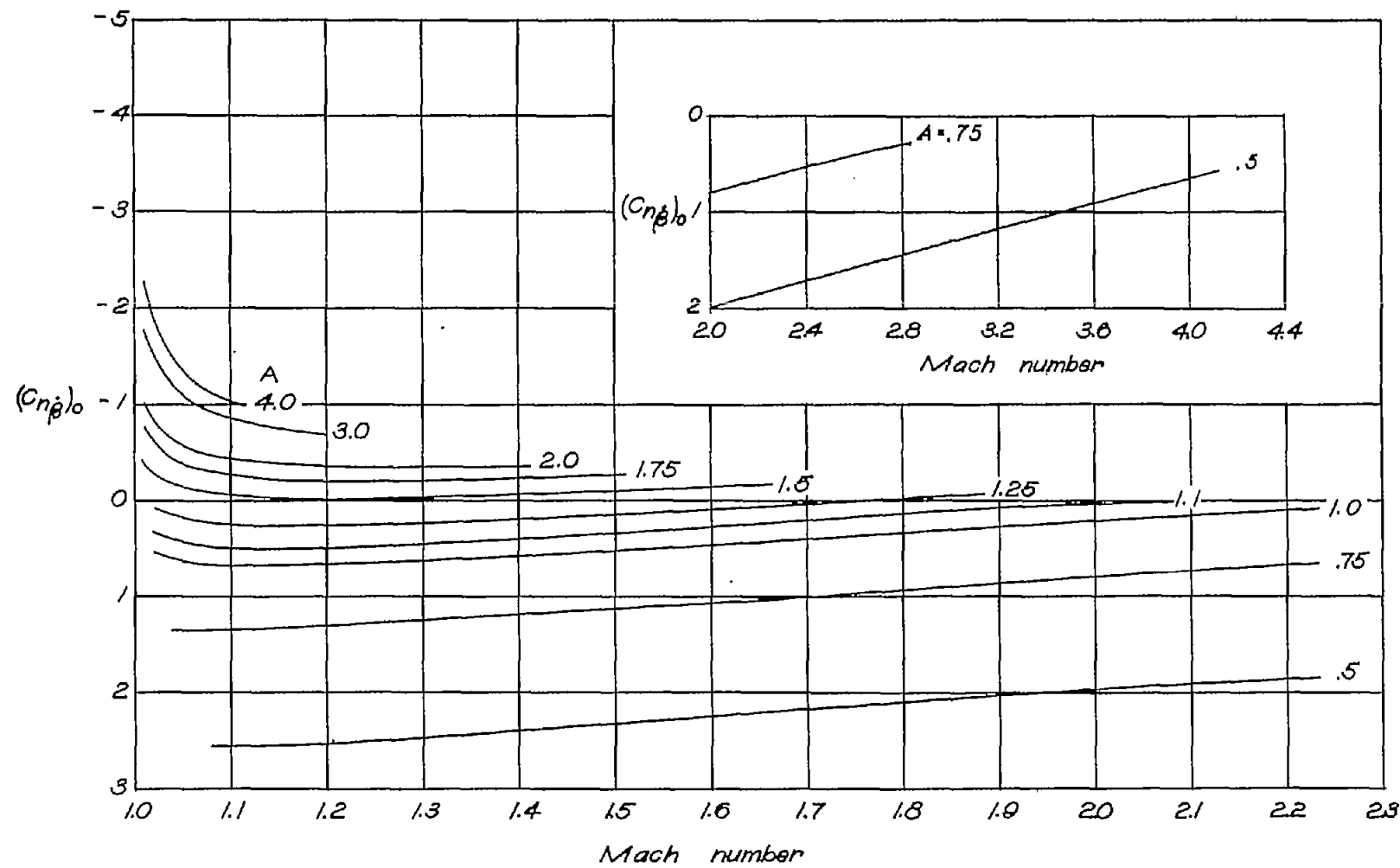


Figure 12.- The variation of $(C_{n\beta})_0$ with Mach number for a number of aspect ratios of a half-delta tail.

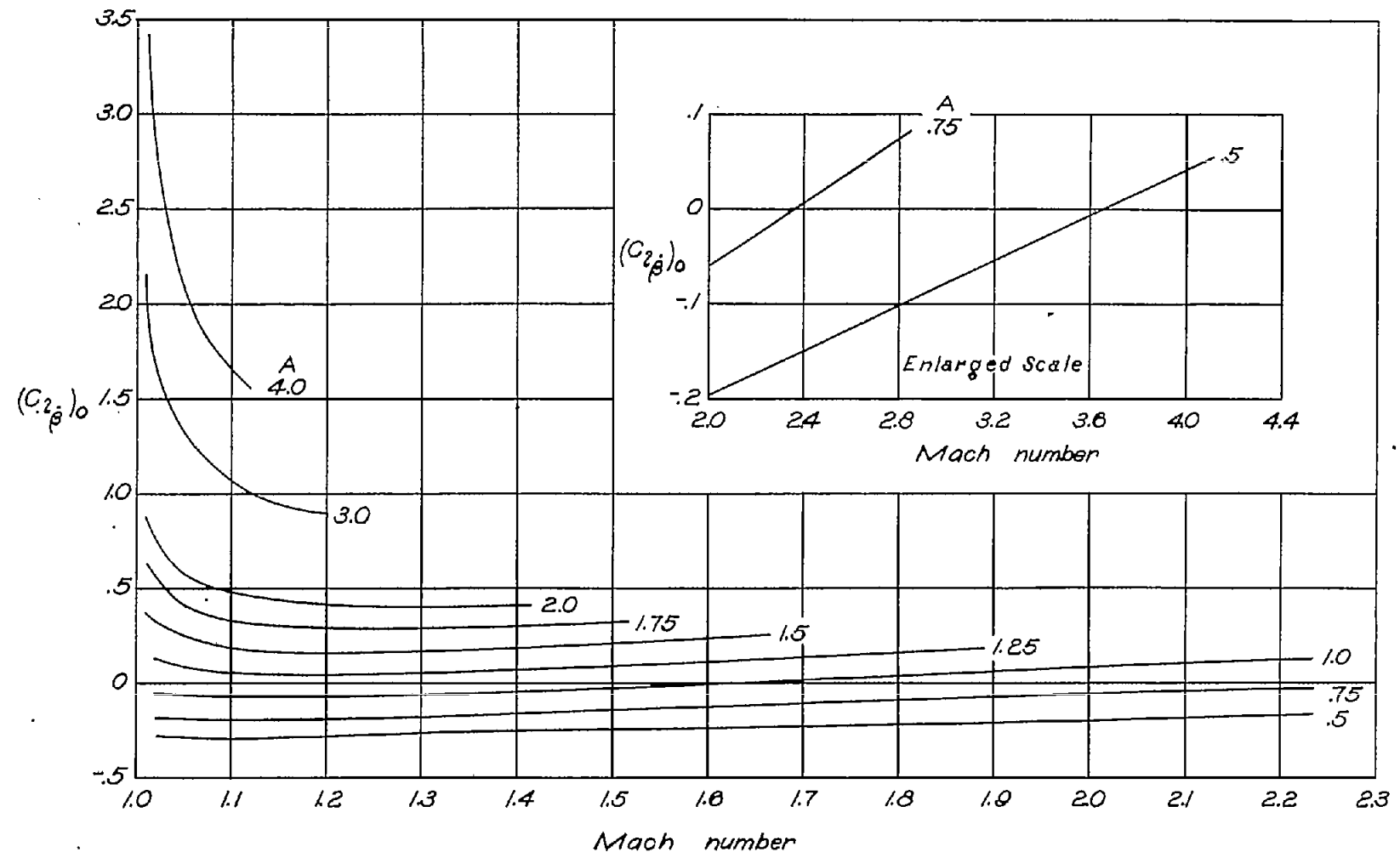


Figure 13.- The variation of $(C_{l\beta})_0$ with Mach number for a number of aspect ratios of a half-delta tail.

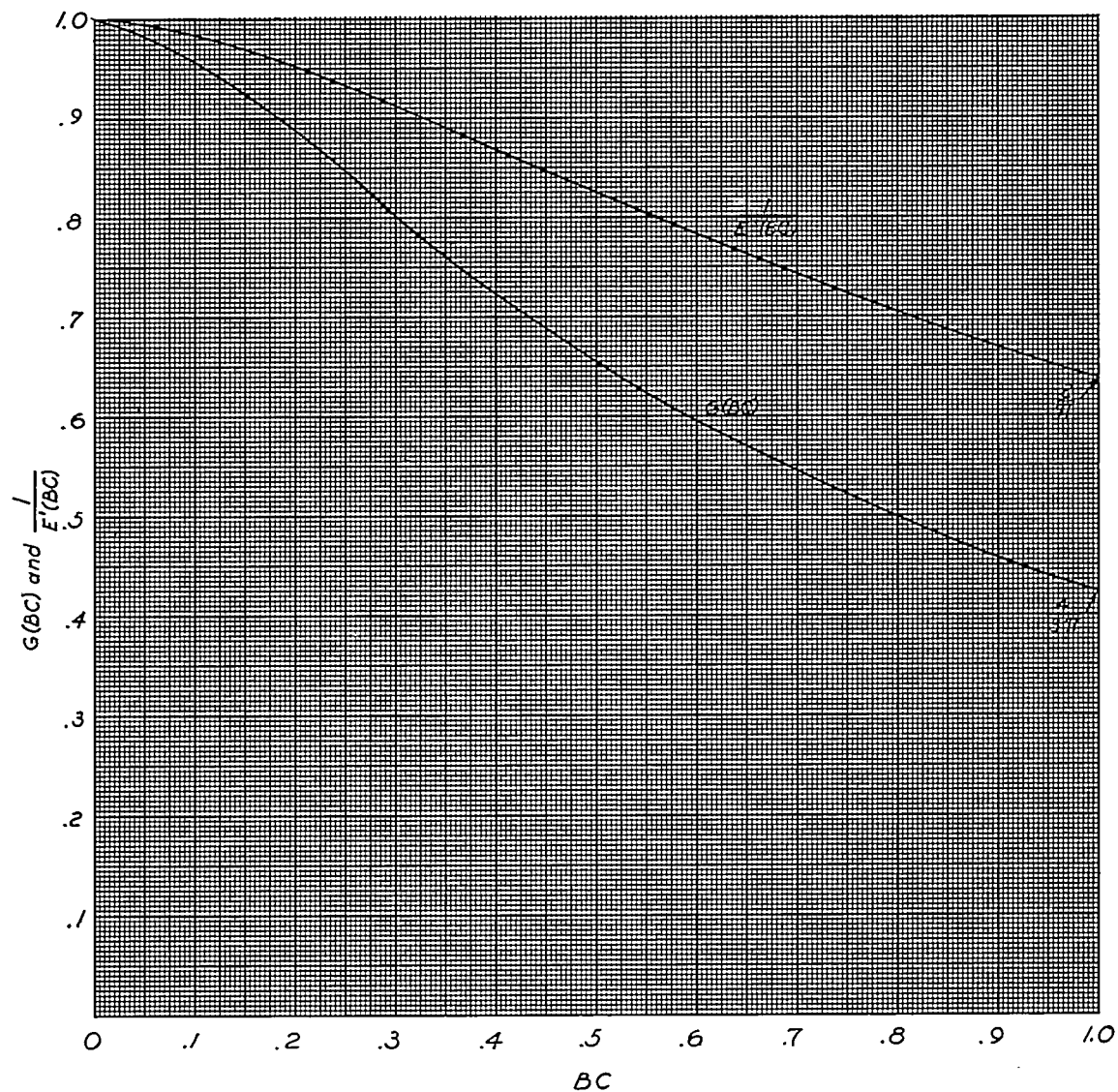


Figure 14.- Variation of the parameters $1/E'(BC)$ and $G(BC)$ with BC . These curves are of use in computing the complete-end-plate stability derivatives given in tables III and IV.

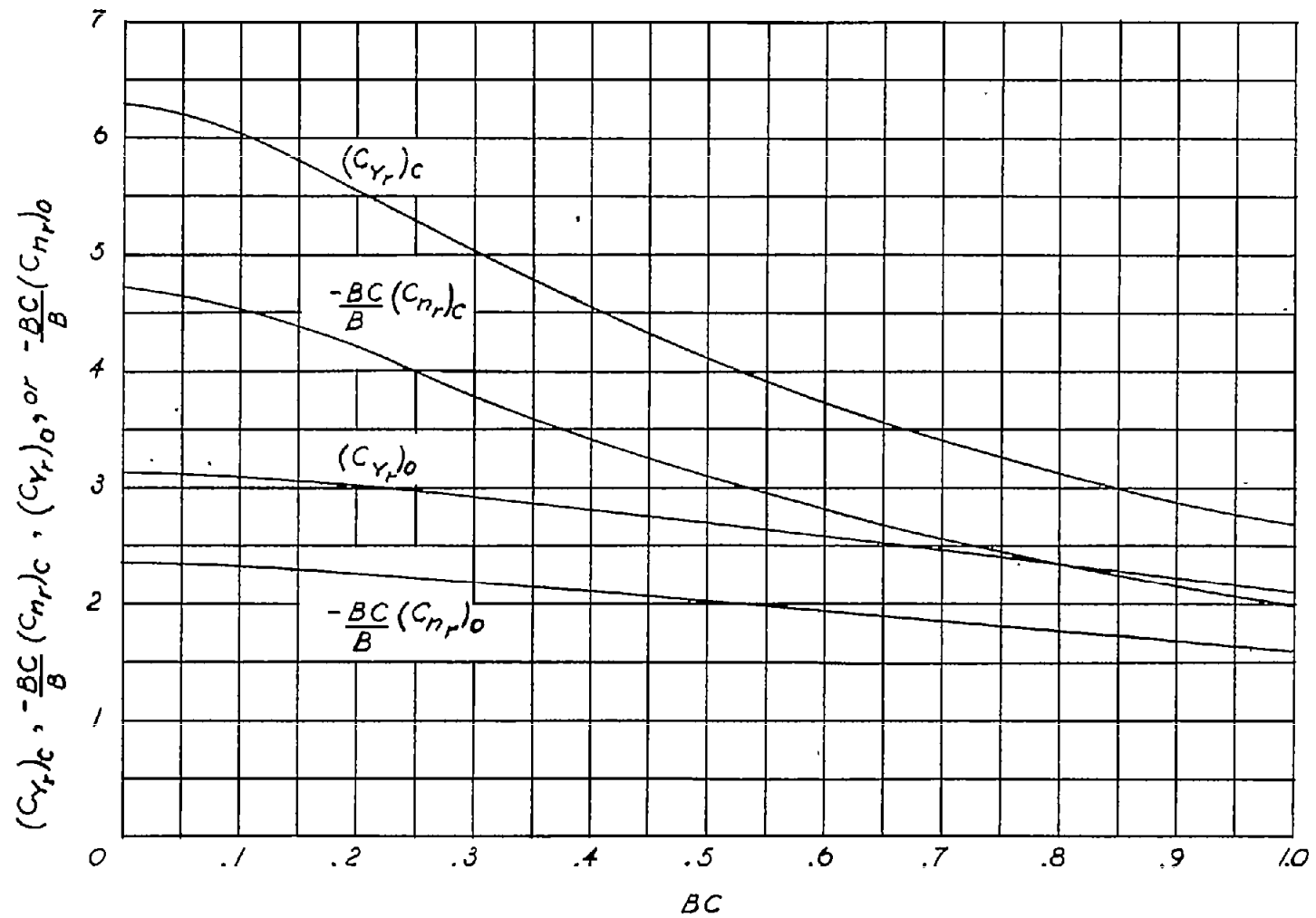


Figure 15.- Complete-end-plate and no-end-plate boundaries of the stability derivative C_{Y_r} and the stability-derivative parameter $-\frac{BC}{B} C_{n_r}$.

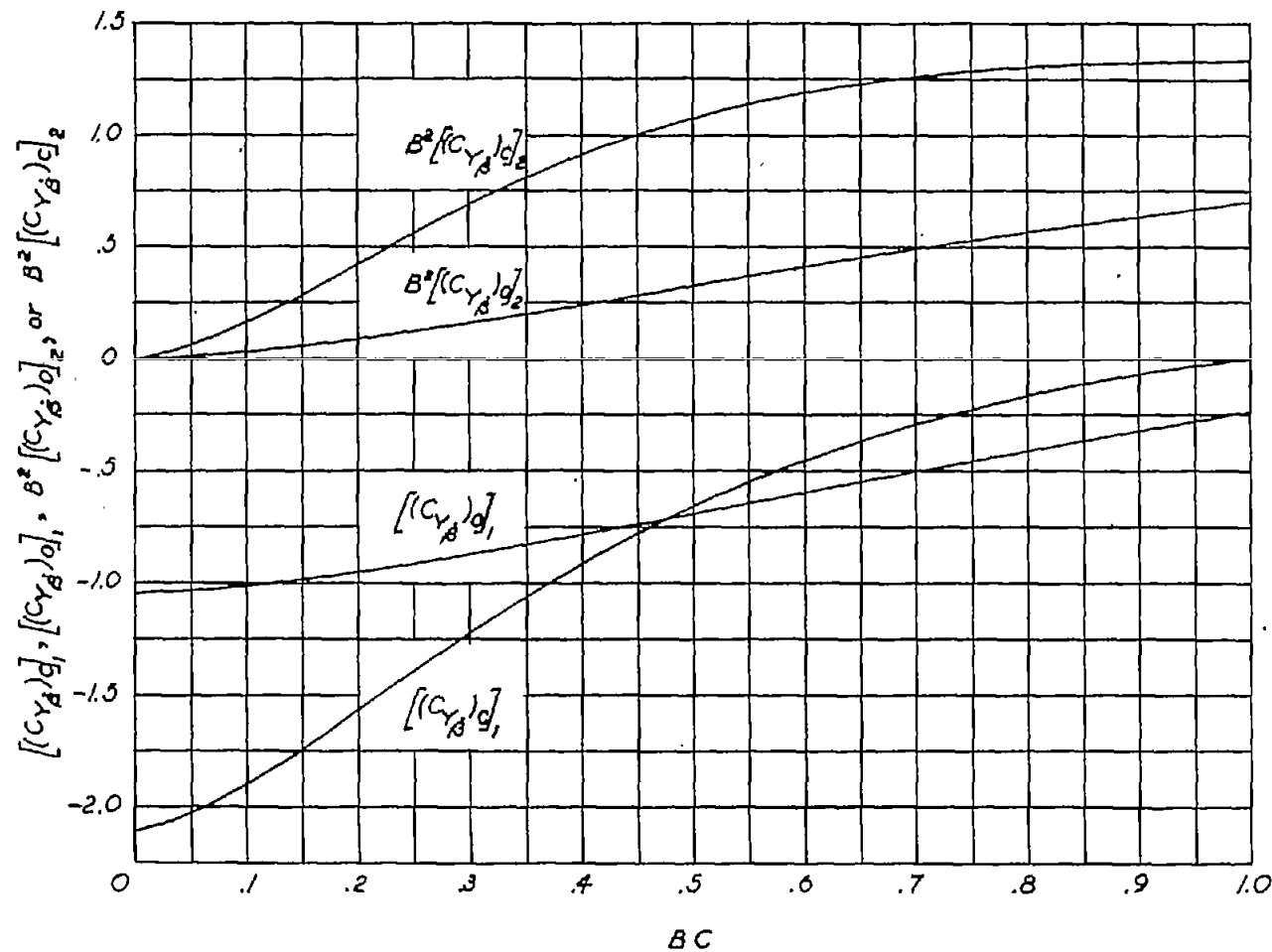


Figure 16.- Complete-end-plate and no-end-plate boundaries of the quantities $B^2[(C_{Y_B})_2]$ and $[(C_{Y_B})_1]_1$. Note that the derivative $C_{Y_B}^*$ is given by the sum of $[(C_{Y_B})_1]_1$ and $[(C_{Y_B})_1]_2$.

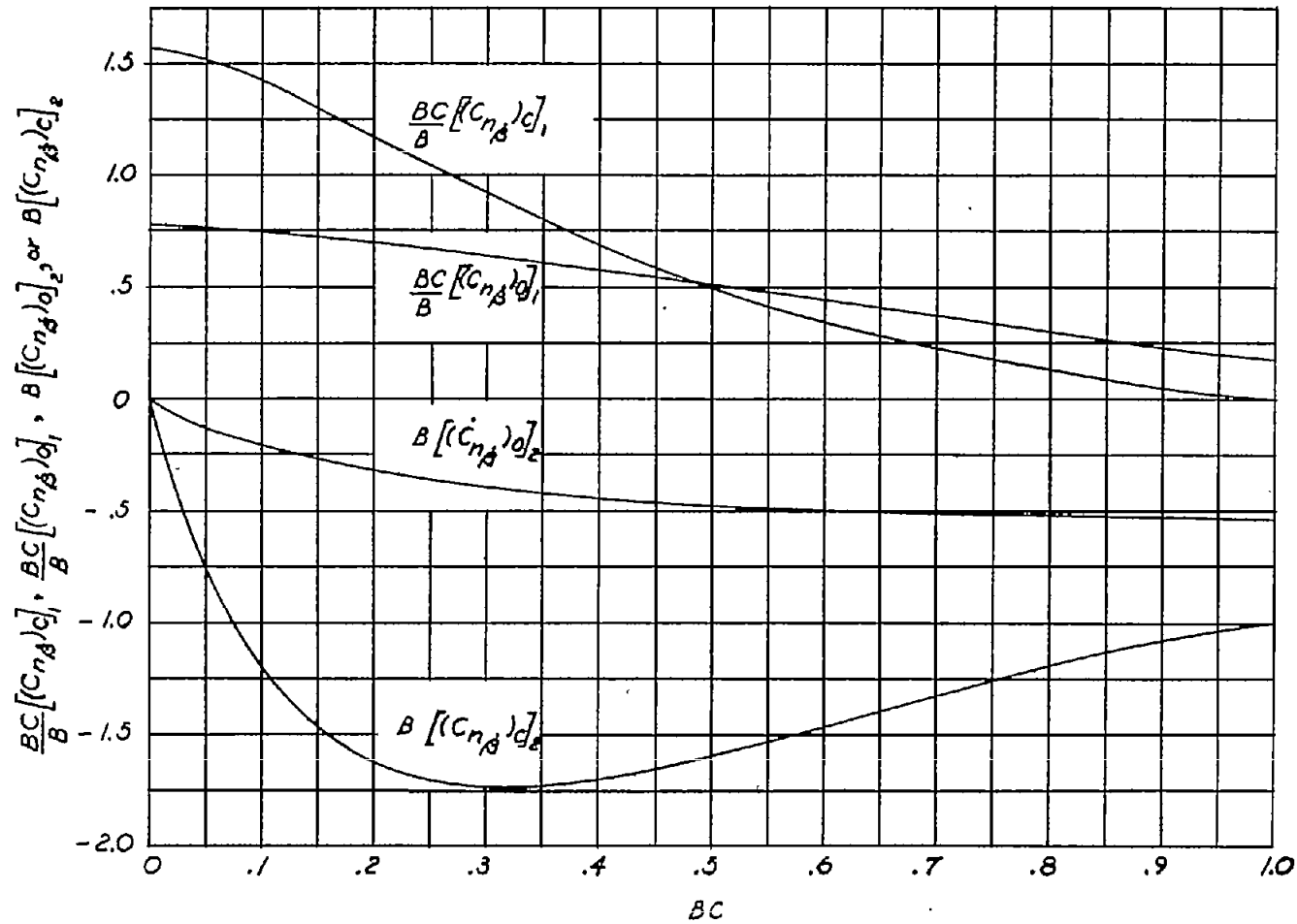


Figure 17.- Complete-end-plate and no-end-plate boundaries of the quantities $B[(C_{n_\beta})_d]_2$ and $\frac{BC}{\delta} [(C_{n_\beta})_d]_1$. Note that the derivative C_{n_β} is given by the sum of $[(C_{n_\beta})_d]_1$ and $[(C_{n_\beta})_d]_2$.

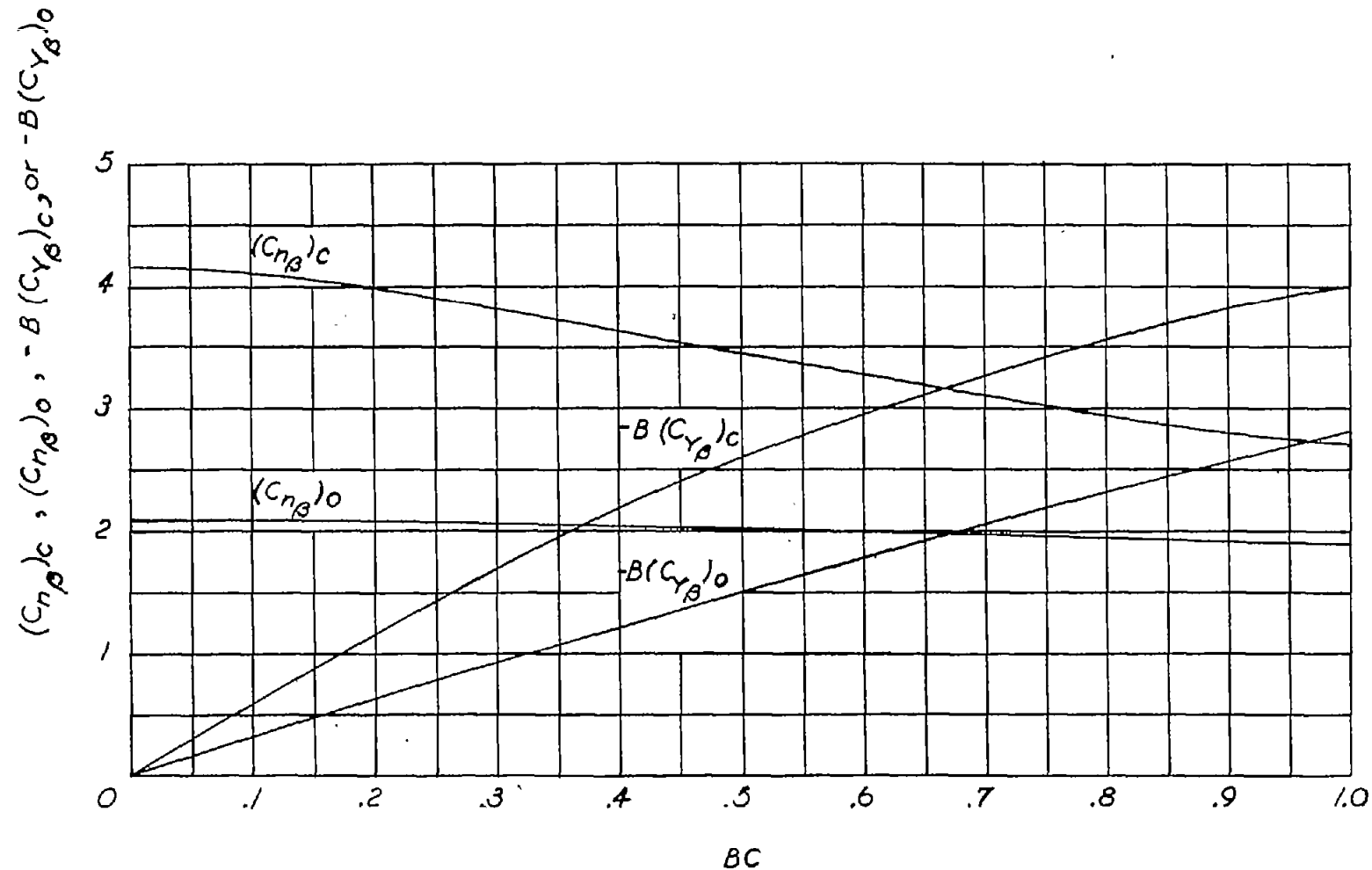


Figure 18.- Complete-end-plate and no-end-plate boundaries of the stability derivative C_{n_B} and the stability-derivative parameter $-B(C_{Y_B})_0$.

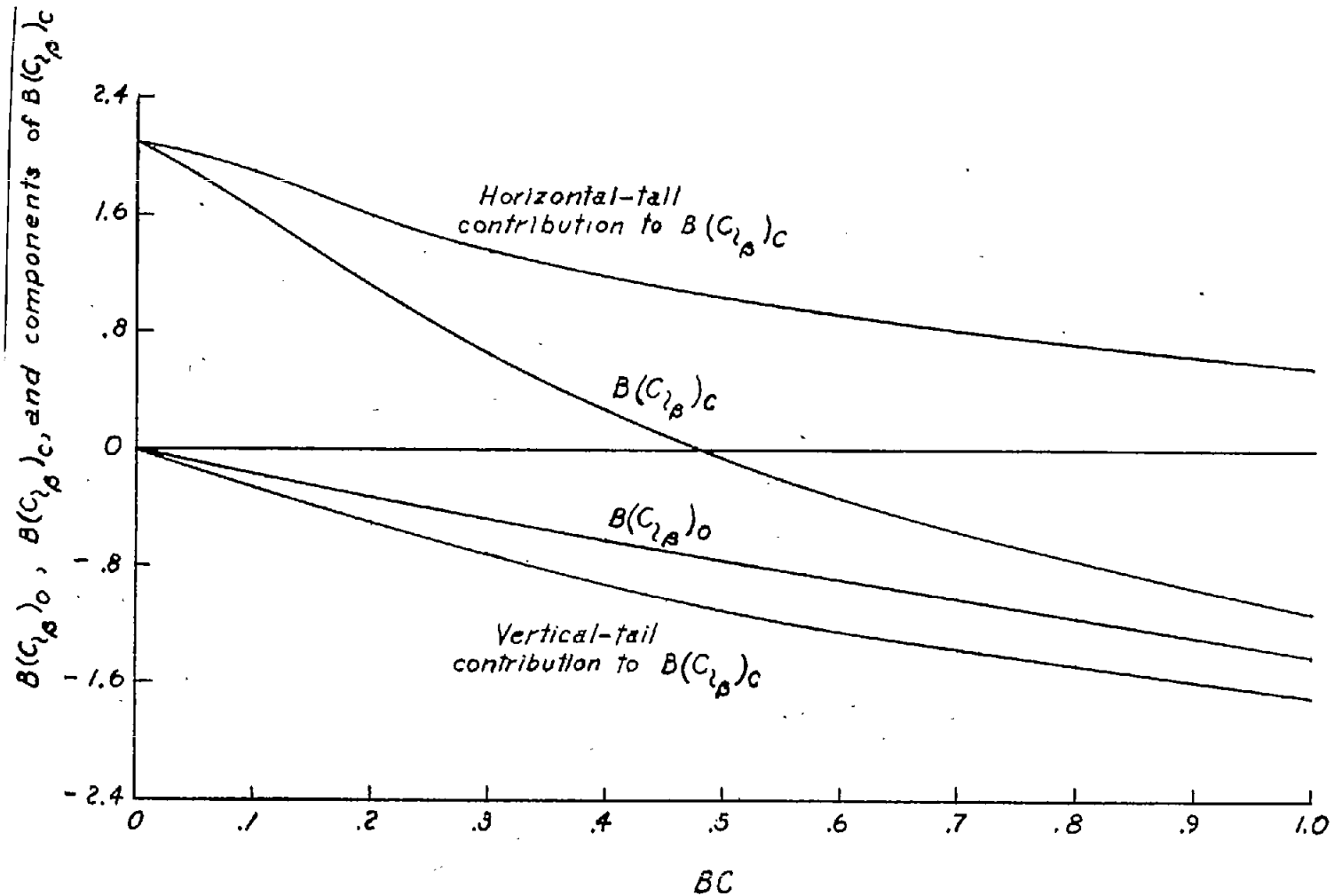


Figure 19.- Variation of $B(C_{l\beta})_0$, $B(C_{l\beta})_C$, and the horizontal- and vertical-tail contributions to $B(C_{l\beta})_C$ with BC .

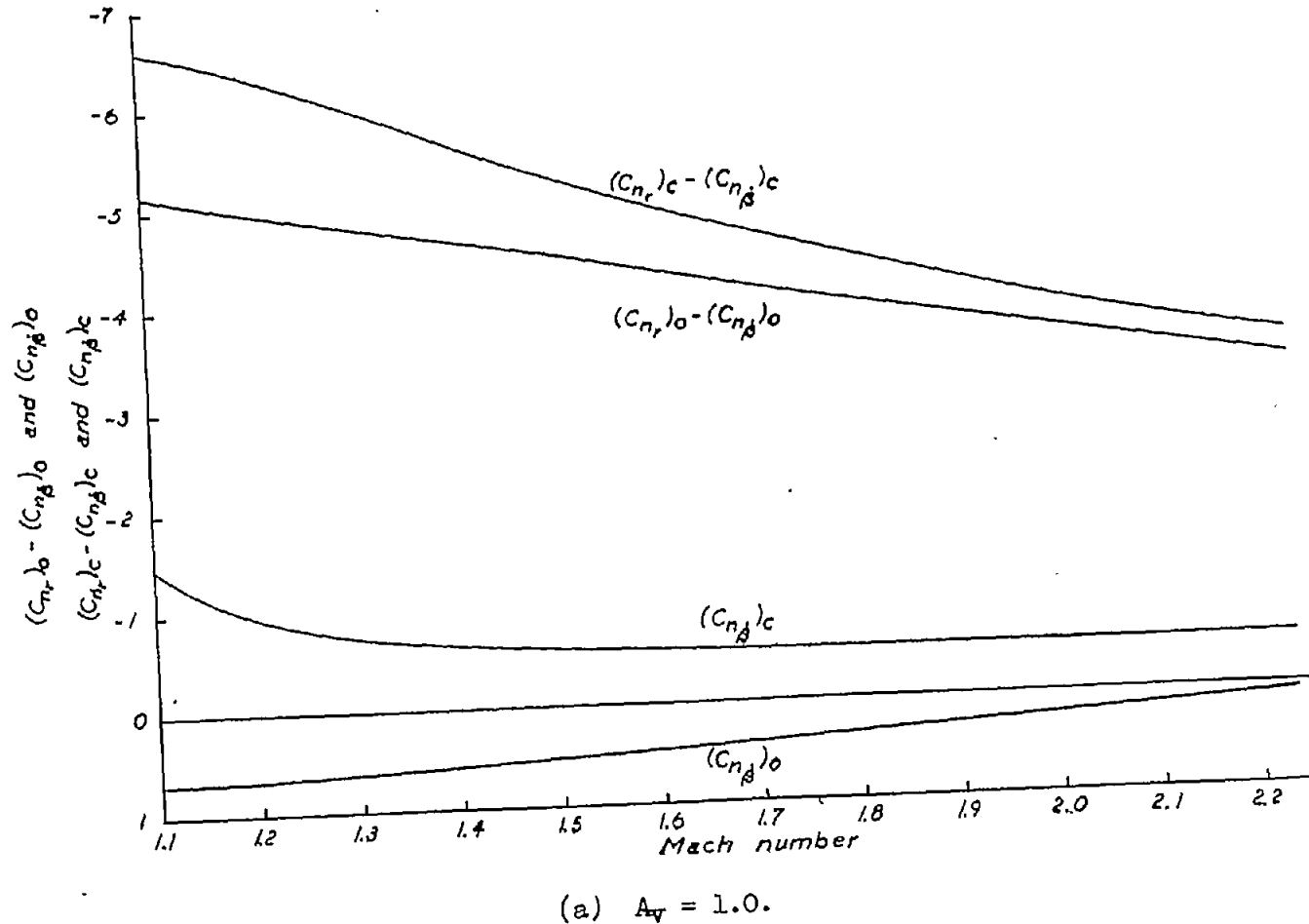


Figure 20.- The variation with Mach number of the first-order approximation to the damping of the lateral oscillation in yaw for complete- and no-end-plate half-delta tails with aspect ratios of 1.0, 1.5, and 2.0. The yawing axis is located at the tail apex.

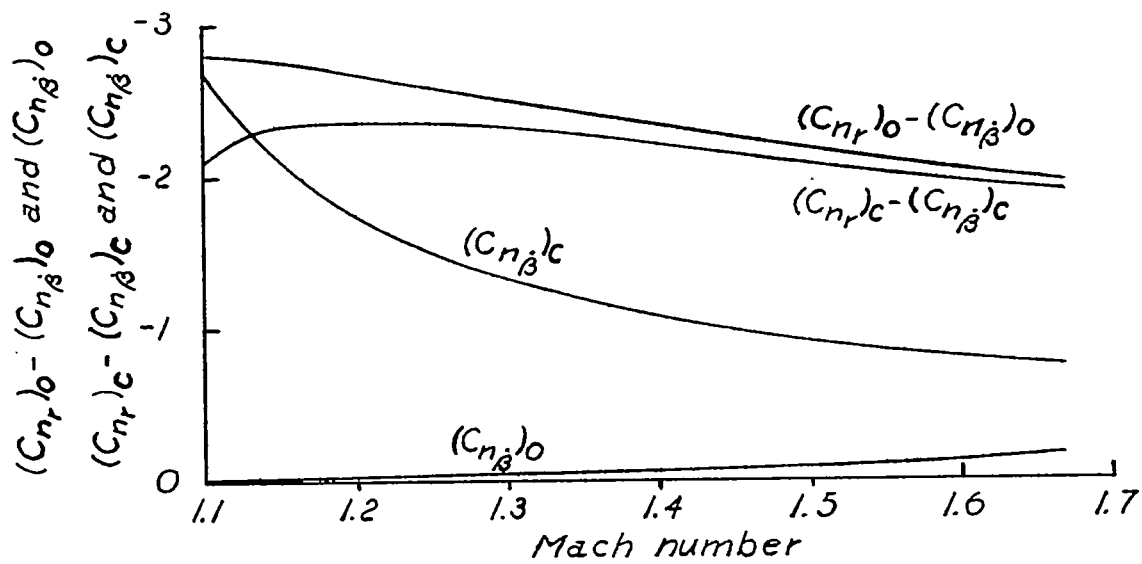
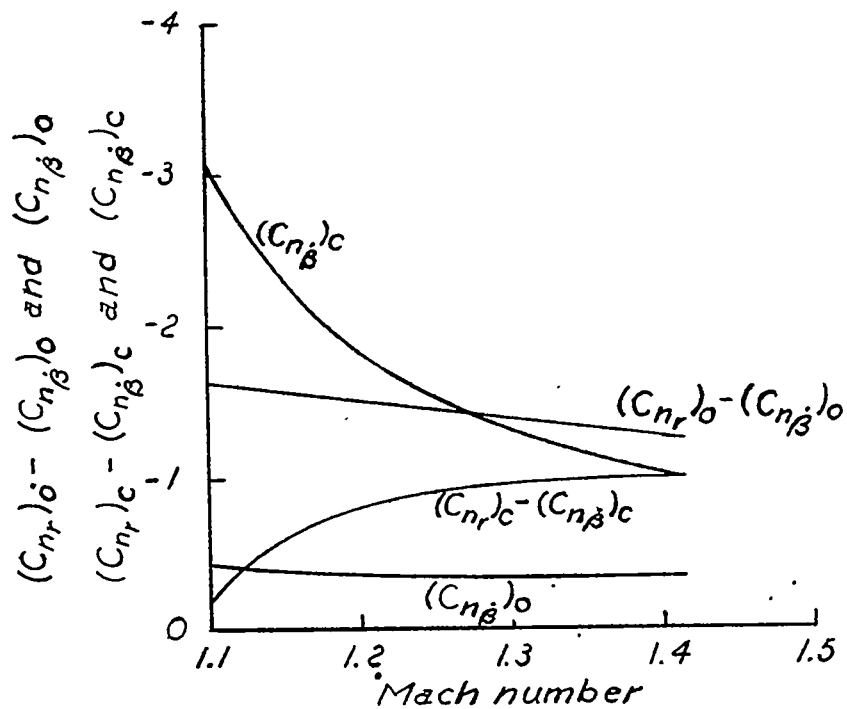
(b) $A_V = 1.5.$ (c) $A_V = 2.0.$

Figure 20.- Concluded.

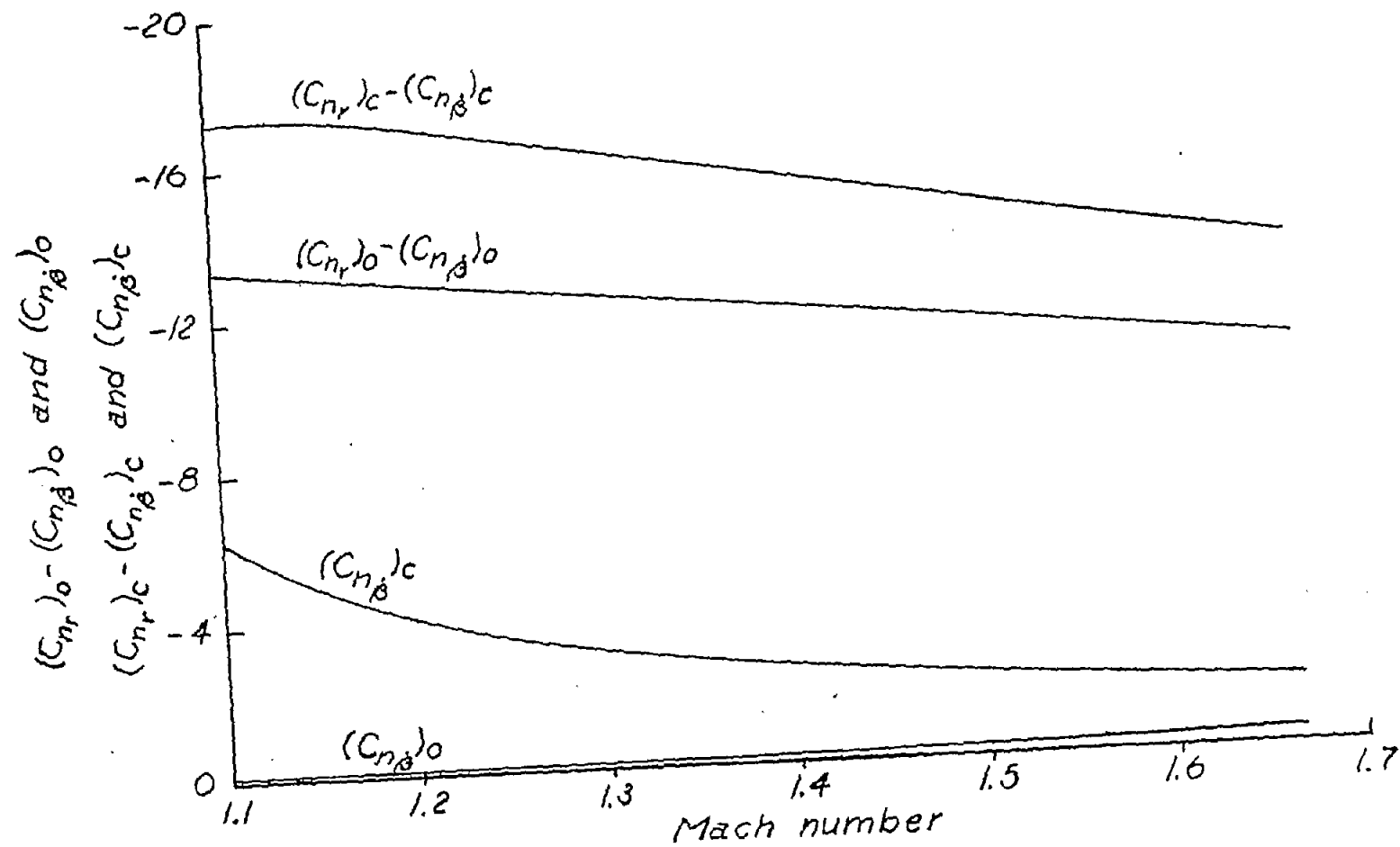


Figure 21.- The variation with Mach number of the first-order approximation to the damping of the lateral oscillation in yaw for a complete- and a no-end-plate half-delta tail of aspect ratio 1.5. The yawing axis is located 1 chord ahead of the tail apex.